CRREL REPORT 78-23

Influence of freezing and thawing on the resilient properties of a silt soil beneath an asphalt concrete pavement

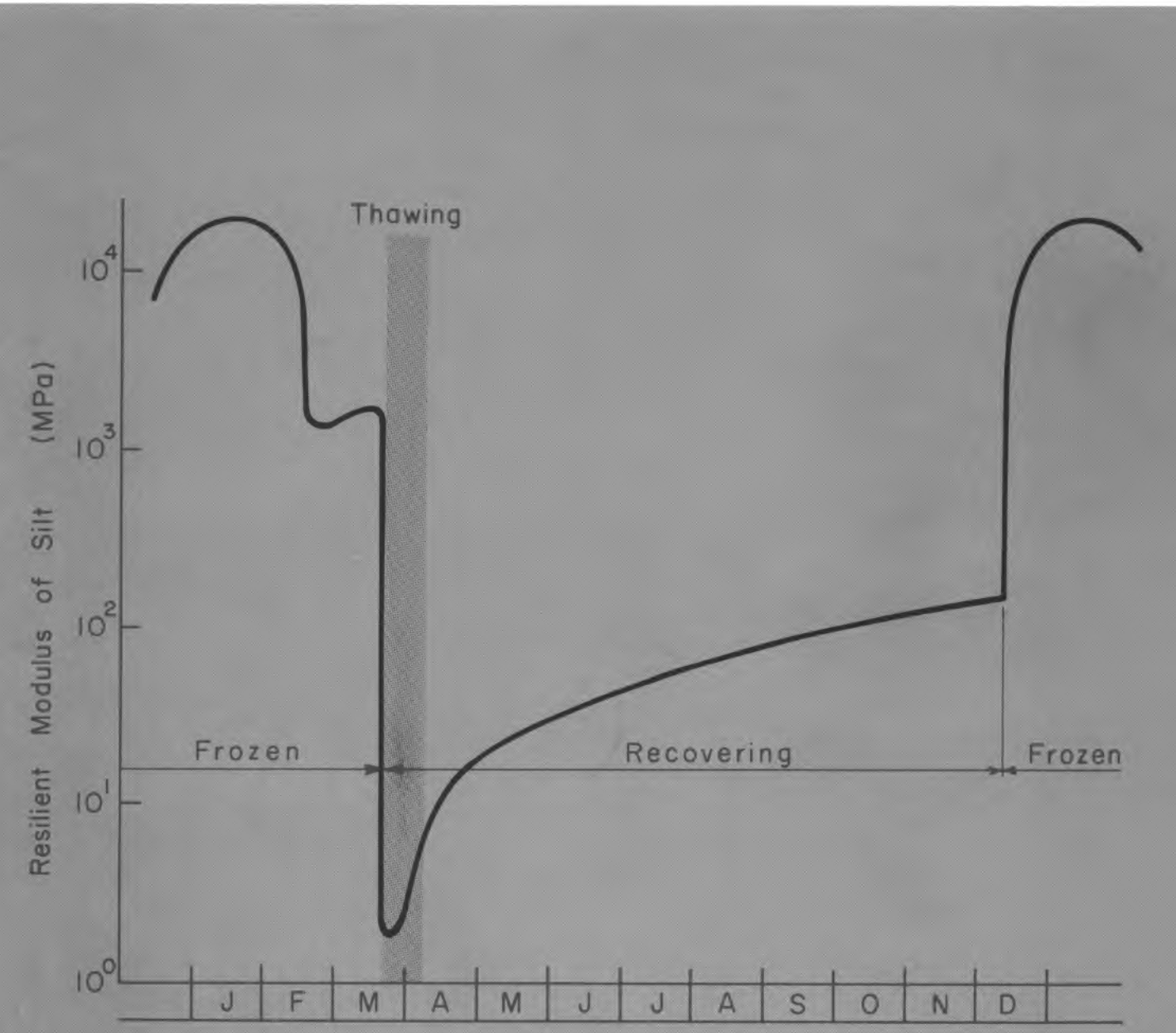

CRREL Report 78-23

Influence of freezing and thawing on the resilient properties of a silt soil beneath an asphalt concrete pavement

T.C. Johnson, D.M. Cole and E.J. Chamberlain

September 1978

Prepared for
DIRECTORATE OF MILITARY CONSTRUCTION
OFFICE, CHIEF OF ENGINEERS
By
COLD REGIONS RESEARCH AND ENGINEERING LABORATORY
U.S. ARMY CORPS OF ENGINEERS
HANOVER, NEW HAMPSHIRE

Unclassified

SECURITY CLASSIFICATION OF THIS PAGE *(When Data Entered)*

REPORT DOCUMENTATION PAGE

READ INSTRUCTIONS BEFORE COMPLETING FORM

1. REPORT NUMBER: CRREL Report 78-23	2. GOVT ACCESSION NO.
3. RECIPIENT'S CATALOG NUMBER	
4. TITLE *(and Subtitle)*: INFLUENCE OF FREEZING AND THAWING ON THE RESILIENT PROPERTIES OF A SILT SOIL BENEATH AN ASPHALT CONCRETE PAVEMENT	5. TYPE OF REPORT & PERIOD COVERED
	6. PERFORMING ORG. REPORT NUMBER
7. AUTHOR(s): T.C. Johnson, D.M. Cole and E.J. Chamberlain	8. CONTRACT OR GRANT NUMBER(s)
9. PERFORMING ORGANIZATION NAME AND ADDRESS: U.S. Army Cold Regions Research and Engineering Laboratory, Hanover, New Hampshire 03755	10. PROGRAM ELEMENT, PROJECT, TASK AREA & WORK UNIT NUMBERS: DA Project 4A762730AT42, Task A2, Work Unit 002
11. CONTROLLING OFFICE NAME AND ADDRESS: Directorate of Military Construction, Office, Chief of Engineers, Washington, D.C. 20314	12. REPORT DATE: September 1978
	13. NUMBER OF PAGES: 53
14. MONITORING AGENCY NAME & ADDRESS *(if different from Controlling Office)*	15. SECURITY CLASS. *(of this report)*: Unclassified
	15a. DECLASSIFICATION/DOWNGRADING SCHEDULE

16. DISTRIBUTION STATEMENT *(of this Report)*

Approved for public release; distribution unlimited.

17. DISTRIBUTION STATEMENT *(of the abstract entered in Block 20, if different from Report)*

18. SUPPLEMENTARY NOTES

19. KEY WORDS *(Continue on reverse side if necessary and identify by block number)*

Asphalt	Repeated-load plate-bearing tests
Concrete	Repeated-load triaxial tests
Elastic properties	Soils
Freezing	Thawing
Pavements	

20. ABSTRACT *(Continue on reverse side if necessary and identify by block number)*

Stress-deformation data for silt subgrade soil were obtained from in-situ tests and laboratory tests, for use in mechanistic models for design of pavements affected by frost action. Plate-bearing tests were run on bituminous concrete pavements constructed directly on a silt subgrade, applying repeated loads to the pavement surface while the silt was frozen, thawing, thawed, and fully recovered. Repeated-load laboratory triaxial tests were performed on the silt in the same conditions. Analysis of deflection data from the in-situ tests showed resilient moduli of the silt as low as 2000 kPa for the critical thawing period, and 100,000 kPa or higher when silt was fully recovered. Analysis of the laboratory tests, which gave moduli comparable to the latter values, showed that resilient modulus

DD FORM 1473 EDITION OF 1 NOV 65 IS OBSOLETE

Unclassified

20. Abstract (cont'd)

during recovery from the thaw-weakened condition can be modeled as a function of the changing moisture conter

PREFACE

This report was prepared by T.C. Johnson, Civil Engineer, Civil Engineering Research Branch, and D.M. Cole, Research Civil Engineer, and E.J. Chamberlain, Research Civil Engineer, Applied Research Branch, Experimental Engineering Division, U.S. Army Cold Regions Research and Engineering Laboratory.

The study was funded under DA Project 4A762730AT42, *Design, Construction and Operations Technology for Cold Regions*; Task A2, *Soils and Foundations Technology/Cold Regions*; Work Unit 002, *Seasonal Change in Strength and Stiffness of Soils and Base Courses.*

Many persons at CRREL participated in this research project, furnished essential support, and contributed to its successful completion. The authors wish to acknowledge particularly the contributions of R. Perham, who developed the repeated-load plate-bearing testing device; J. Stubstad and N. Smith, who modified and adapted various components of the test equipment, developed the testing procedures, and performed most of the plate-bearing tests; R. Eaton, who took samples and ran some of the plate-bearing tests; and D. Van Pelt, who reduced the data and assisted with the computer analyses.

This report was technically reviewed by F.D. Haynes and W.F. Quinn of CRREL.

CONTENTS

ILLUSTRATIONS

TABLES

NOMENCLATURE

R^2	correlation coefficient
S	degree of saturation, %
T	temperature, °C
M_r	resilient modulus, Pa
w	moisture content, %
γ_d	dry unit weight, g/m^3
ϵ_a	axial unit strain, dimensionless
ϵ_r	radial unit strain, dimensionless
μ_r	resilient Poisson's ratio, dimensionless
σ_1	major principal stress, Pa
σ_3	minor principal stress, Pa
σ_d	deviator stress, Pa
θ	sum of principal stresses, Pa

CONVERSION FACTORS: METRIC (SI) TO U.S. CUSTOMARY UNITS OF MEASUREMENT

Multiply	*By*	*To obtain*
millimeter	0.039370	inch
meter	3.280840	foot
kilogram	2.204622	pound
kilonewtons	224.8089	pound force
kilogram/meter^3	0.062428	pound/foot^3
megagram/meter^3	62.42797	pound/foot^3
kilopascal	0.145038	pound force/inch^2
megapascal	145.0377	pound force/inch^2
gigapascal	145037.7	pound force/inch^2
degrees Celsius	$t_{°F} = 1.8t_{°C} + 32$	degrees Fahrenheit

INFLUENCE OF FREEZING AND THAWING ON THE RESILIENT PROPERTIES OF A SILT SOIL BENEATH AN ASPHALT CONCRETE PAVEMENT

T.C. Johnson, D.M. Cole and E.J. Chamberlain

INTRODUCTION

In the past the design of pavements in the cold regions has relied upon a single index of subgrade supporting capacity, whose numerical value is selected to represent the worst case during thawing, the normal case after recovery, or some sort of annual average (Johnson et al. 1975). In recent years the need for more adequate accounting for the extreme seasonal variation in subgrade supporting capacity has been recognized and design methods based on calculated stresses and strains have been developed.

As these mechanistic design methods become more widely adopted and refined, it will be possible to render such an accounting by incorporating in the method a damage accumulator. This approach will permit the pavement damage occurring in each season to be calculated and summed to represent the total yearly damage caused by traffic. A trial pavement design could then be adopted if the total damage accumulation during the selected number of years of economic life were within limits determined in relation to desired pavement serviceability. Effective application of a cumulative damage approach, however, requires that the actual properties of subgrade soils in each season be determined.

Design procedures are available (Bergan and Monismith 1972, Barker and Brabston 1974) for analysis of damage accumulation in pavements subjected to freezing and thawing. These methods require a prediction of the seasonal values of the resilient modulus M_r (total stress divided by recoverable strain), and resilient Poisson's ratio μ_r, of each type of soil, base course, or other material in the pavement profile.

The objective of the research summarized herein was to develop reliable laboratory testing techniques for obtaining M_r for silts, which are known to exhibit a large seasonal range in supporting capacity. The approach was to determine the resilient modulus of a silt subgrade soil in the frozen, thawing, and recovery conditions by means of field in-place tests, and then to develop techniques for laboratory tests that would yield similar moduli for the same material. A further objective of the laboratory tests was to obtain data from which Poisson's ratio could be calculated.

SELECTION OF EXPERIMENTAL APPROACH

Previous investigations of effect of freeze-thaw on soil deformability

Numerous research investigations of the resilient properties of soils and paving materials have been conducted since Seed et al. (1955) established the concept of modulus of resilient deformation as the applied stress divided by the recoverable strain. While the effects of significant variables such as moisture content, density, and magnitude of repeatedly applied stress have been evaluated in many studies, the most critical factor affecting the resilient modulus of fine-grained subgrade soils for pavements in cold regions, freeze-thaw cycling, has been less exhaustively studied.

Culley (1970) performed repeated-load triaxial compression tests on compacted specimens of sandy clay (glacial till) having a liquid limit (LL) of 33% and plastic limit (PL) of 16%, and measured resilient and residual strains and resilient moduli. Tests were run on samples merely tempered for seven days after molding, and on samples that had been subjected to three cycles of closed-system freeze-thaw. Freezing was unidirectional, comprising eight hours' exposure of the top of the specimen to a constant temperature of –17.8°C. Specimens were tested undrained, and axial loads were cycled at one per 3 s with a load duration of 0.25 s. The effect of freeze-thaw was found to depend upon the density and moisture content of the specimens; at the optimum moisture content from the T-99 compaction test (AASHTO 1974) the reduction in the modulus caused by freeze-thaw ranged from 41 to 66%, depending on the density. At a moisture content 1.5%

above optimum, and at the maximum density of the AASHTO T-99 test, the modulus changed from 77.6 MPa before freeze-thaw to 21.5 MPa after freeze-thaw.

Mickleborough (1970) made intensive investigations of the effect of freeze-thaw on the resilient properties of a highly plastic glacial lake clay (LL 77, PL 47) compacted to the maximum density of the AASHTO T-99 test. Tests were similar to those reported by Culley (1970) except that resilient moduli were determined for samples subjected to 0, 1, 2 and 4 freeze-thaw cycles, and that closed-system freezing was at temperatures chosen to cause freezing in 24 hours. Typical results at a moisture content of 33% showed resilient moduli of 39.3, 16.5, 14.5 and 10.3 MPa after 0, 1, 2, and 4 cycles of freeze-thaw.

MacLeod (1971) made repeated-load triaxial tests on samples of sandy clay (glacial till) taken undisturbed in the month of October from the subgrade of a road pavement in Saskatchewan that had been in service three years. The degree of saturation of the samples ranged from about 75 to 85%. Samples were tested under axial load cycles applied at the rate of one per 3 s with duration of 0.1 s. During application of repeated loads, the samples were in contact with porous disks that allowed dissipation of air pressures while not permitting water flow, hence allowing accumulation of pore water pressures during testing. After each test the sample was wrapped in plastic film, frozen unidirectionally for 8 hours at -17.8°C, thawed for 8 hours and retested. The results showed a substantial decrease in resilient modulus for the thawed samples, but even at the higher deviator stresses the modulus did not fall below about 35 MPa and in most cases was at least 70 MPa. The same investigation included measurement, with the Benkelman beam, of the surface deflection of the same pavement from which the samples had been taken.

The resilient properties of the materials in the pavement profile were characterized with the help of laboratory tests, and the pavement was analyzed as an elastic layered system to calculate the deflections. The calculated deflection was about 40% less than the measured deflection, and MacLeod postulated that changes in the resilient modulus of the subgrade at shallow depths may have influenced the field deflections, or that the laboratory materials characterization may have overestimated the resilient moduli. The investigation also included resilient modulus testing of several samples of granular materials (base and subbase) after freeze-thaw. The author did not report details of the conditions under which freezing took place, or put forward any conclusions except that the effects of freeze-thaw on the modulus of the granular material were smaller than on that of the subgrade materials.

Pagen and Khosla (1968) studied the rheological properties of a processed kaolin (LL 58, PL 36) after nine cycles of closed-system freeze-thaw. Samples were frozen either directly after compaction and tempering, or after partial saturation to about the plastic limit. Freezing was not unidirectional, and samples were exposed to a temperature of -28.9°C for seven hours, then thawed in the humid room for periods of less than one day to more than two days. For these conditions it was found that varying degrees of saturation up to 80 to 90%, depending on degree of compaction, had little effect on strength and deformability, but that above a certain critical degree of saturation the rheological parameters of the soil decreased rapidly and approached minimum values.

Bergan (1972) made repeated-load triaxial tests on undisturbed samples of the same lacustrine clay tested in the remolded state by Mickleborough (1970). The samples were taken in the fall of 1970 from the subgrade of an asphalt pavement. Confining pressure was a constant 13.8 kPa, and deviator stresses up to 34.4 kPa were cycled once each 3 s, with a duration of 0.1 s. Resilient moduli were in most cases between 35 and 70 MPa, averaging 58 MPa. Some of the samples were then wrapped in plastic and unidirectionally frozen by exposure to a temperature of -17.8°C for 8 hours. After thawing for 8 hours the samples were again tested. The resilient modulus dropped considerably; at 1000 repetitions it ranged generally from 27 to 41 MPa. After continued load repetitions it recovered its original value prior to freeze-thaw. Bergan also used laboratory characterizations of the subgrade and pavement materials as inputs in an analysis of the pavement as an elastic layered system, calculating the deflections under a 40-kN load on dual tires. He found the calculated deflections were slightly less than deflections measured with the Benkelman beam.

Bergan and Monismith (1973) refer to the data on undisturbed specimens sampled in the fall, reported by Bergan (1972), and also present laboratory resilient moduli determined on specimens that were taken undisturbed from the same pavement in the spring of 1972. Resilient moduli averaged 43.4 MPa compared with 56.5 MPa for the fall samples. Tests of remolded samples, compacted to in-situ moisture content (33%) and density, showed resilient moduli of 102 MPa when samples were tested without freeze-thaw and 44.7 MPa for two cycles of closed-system freeze-thaw.

Robnett and Thompson (1976) performed repeated-load triaxial tests on compacted specimens of silty clay (LL 32, PL 23) and lean clay (LL 46, PL 22). Tests were made without freeze-thaw, and after one to ten cycles of freeze-thaw without change in moisture content (closed system). Freeze-thaw was found to have an extreme softening effect on the resilient behavior of the soils. Even though the lean clay had

substantially higher resilient modulus values after compaction than did the silty clay, both soils had similar resilient moduli after freeze-thaw, ranging from about 20 to 40 MPa at varying levels of deviator stress. Similar tests also were run on the same soils treated with 5% hydrated lime. Resilient moduli of compacted specimens were substantially higher than those of the untreated soil, and even after 10 cycles of freeze-thaw the moduli of the treated soils ranged from 96 to 138 MPa.

Selection of laboratory test method

The research mentioned in the previous section has provided valuable information and insight regarding the effect of freeze-thaw on resilient properties of fine-grained soil. The results are of particular interest for road design in Saskatchewan (mean annual precipitation in Regina 400 mm) where much of the research was done, and in other cold mid-continent areas with relatively low rainfall and deep ground water table. Nevertheless, the exclusive use of closed-system conditions in the induced freezing cycles leads one to question whether the numerical results could find extensive useful application in other cold areas with more abundant moisture.

Accordingly, it was decided to investigate the resilient properties of subgrade soils frozen and thawed under the prevailing winter and spring conditions in Hanover, New Hampshire (mean annual precipitation 925 mm). The first soil selected for study was a silt of very low plasticity, for which the test results are presented here. It was decided to determine the resilient properties of the material by means of repeated-load triaxial tests, which would permit adequate control of stress state and would yield both resilient modulus and Poisson's ratio. A major weakness of these tests, however, is that meaningful results can be obtained only on fully frozen or fully thawed specimens, and the critical condition *during* thawing cannot be investigated. Therefore, consideration was given initially to use of a laboratory repeated-load plate bearing test, which could include application of loads while the thaw front continued to advance more deeply into the specimen. But while the stressed zone in such a test would include the thaw front, as it does under traffic loading on a pavement during thawing of its subgrade, the need to determine Poisson's ratio by other means to analyze the results, as well as the larger specimens that would be needed, and the unknown effect of the specimen container on the plate deflections led to a decision in favor of the triaxial compression test.

Selection of method of field validation tests

Inherent in the selected laboratory testing method are several conditions and testing variables that it was felt could significantly affect the results, and consequently a suitable field validation of the laboratory characterization of the resilient properties was essential. Two methods of field testing of an experimental pavement were considered: Benkelman beam tests and repeated-load plate-bearing tests. In either case the primary pavement response to be observed was surface deflection, from which the subgrade resilient modulus could be calculated by means of an elastic layered system analysis. Each test offered certain advantages.

The Benkelman beam test, measuring the rebound deflection of the pavement as one set of dual tires of a loaded truck moves away from the test point, has the important advantage of simplicity. Application of load through a truck tire rather than a rigid steel plate also is advantageous; not only is it identical to the loading medium on a pavement in normal service, but being a flexible medium, it closely approaches one of the basic assumptions of the elastic layered system analysis, that the load be uniformly distributed over a circular area. The plate-bearing test is at a disadvantage in the latter regard, because the condition of uniform deflection of the rigid plate underlain by cohesive soil causes higher stresses to develop beneath the edges of the plate than beneath the central part.

The principal advantage of the repeated-load plate-bearing test is that the loading and unloading times and the pulse duration can be controlled accurately. In the rebound procedures of the Benkelman beam test the time of loading is uncertain, but has been estimated by Bergan (1972) as 1 to 10 s. As a controlled loading time for the laboratory triaxial tests was desired, approximating low-speed traffic, and it was considered essential that the field validation tests employ the same load pulse, the repeated-load plate bearing test was selected.

It was realized that the elastic layered system analysis might somewhat overestimate the deflections of a rigid plate, and that the inherent assumption that the bottom layer extends vertically to infinity would further exaggerate the calculated deflections. Hicks (1970) stated that the surface deflection for the same load would be about 20% less under a rigid plate than under a flexible plate. In comparing the deflections computed by methods that assume, on the one hand, a flexible plate and, on the other, a rigid plate, Hicks found that an assumption of a load condition intermediate between perfectly rigid and perfectly flexible plates would have given deflections that predicted more closely those actually measured in plate-bearing tests.

Hicks' studies showed nevertheless, that the elastic layered system analysis predicted the deflections measured in plate-bearing tests reasonably well. Consequently, it was believed the non-uniform pressure distribution beneath the plate, and the deviation of the bottom layer from the assumed semi-infinite extent, would not grossly invalidate the calculation of moduli by means of that type of analysis.

FIELD REPEATED-LOAD PLATE-BEARING TESTS

Test pavements, soils and materials

Repeated-load plate-bearing tests were performed from February to December 1975, at six test points on two pavements constructed in Hanover, New Hampshire, in July 1971. The pavements are entirely of asphalt concrete, placed directly on a prepared subgrade (Eaton and Van Pernis 1973); the thickness of asphalt concrete is 127 mm for one pavement and 229 mm for the other (Fig. 1).

The subgrade soil is a silt of very low plasticity containing varying amounts of sand (Fig. 2), classified ML under the Unified Soil Classification System. The soil is considered extremely frost-susceptible, as evidenced by significant moisture migration and frost heave even in closed-system freezing (Quinn et al. 1973), and by frost heave and spring breakup problem experienced on roads in Hanover constructed on similar materials.

After thoroughly scarifying and blending the top 0.45 m, the subgrade was recompacted and the first layer of asphalt concrete binder course was placed directly on the silt. The mix design for the binder course used throughout both the 127-mm and 229-mm pavements, except in the 38-mm surface course, was determined by the Marshall method (Table I). The job-mix formula prescribed by the New Hampshire Department of Public Works for surface course was used in the top 38 mm of both pavements.

Asphalt concrete for both the 127-mm and 229-mm pavements was prepared from crushed stone aggregates from Lebanon, New Hampshire, and 85-100 penetration asphalt. Pertinent properties of the asphalt and aggregates were determined from core samples taken from the pavements in 1975, four years after construction (Table II and Fig. 3).

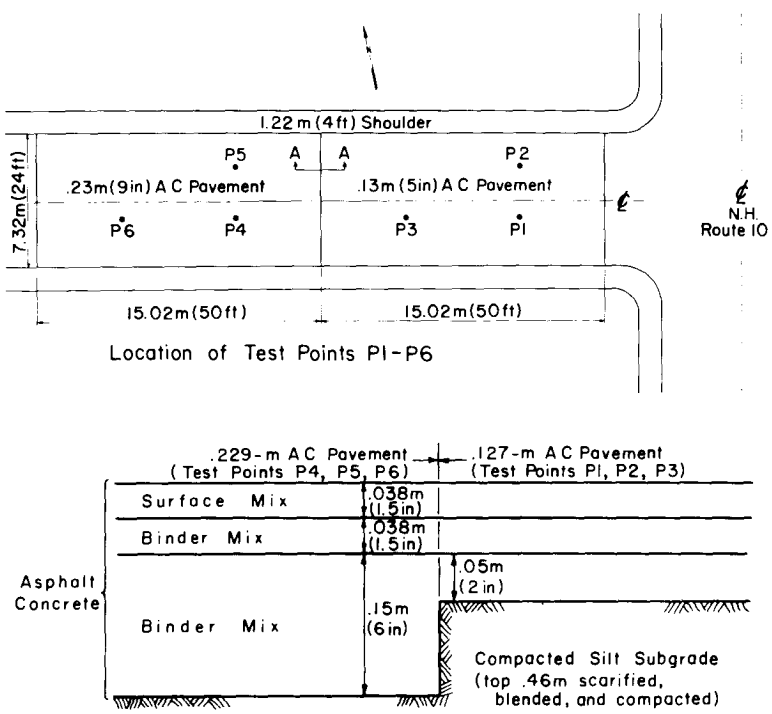

Figure 1. Test pavements.

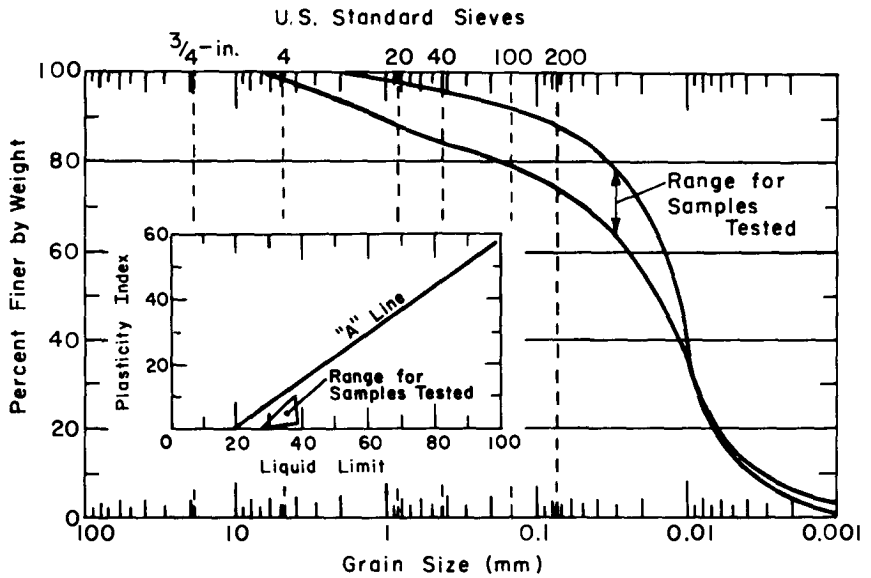

Figure 2. Properties of silt.

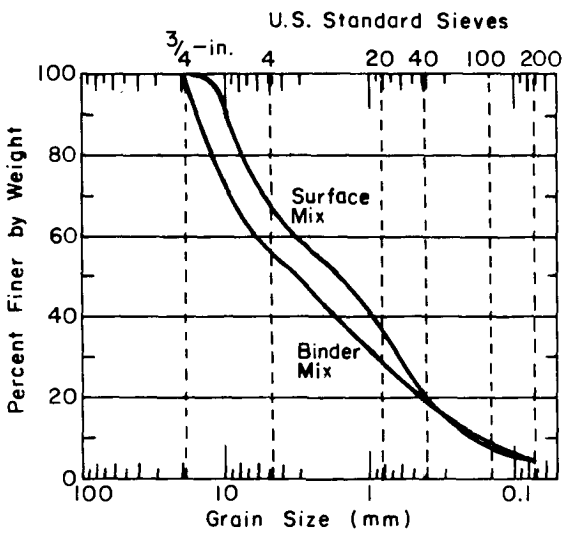

Figure 3. Aggregates for asphalt concrete.

Table I. Marshall properties of binder course.

Asphalt content	4.3%
Stability	780 kg (1720 lb)
Flow	1.02 mm (.04 in.)
Voids total mix	4.8%
Voids filled	70.0%
Density	2440 kg/m^3 (152.6 lb/ft^3)

Table II. Properties of extracted asphalt.

Source	*Asphalt content (%)*	*Pen. (100 g, 25°C)*	*Softening point (°C)*	*Absolute viscosity, 60°C Pa·s (poises)*	*Kinematic viscosity, 135°C m^2/s (centistokes)*	*Pen-Vis number (after McLeod 1972)*
Surface mix	5.9	45	54.6	567 (5670)	5.70 (570)	–0.6
Binder mix	5.5	65	50.5	232 (2320)	4.41 (441)	–0.5

Figure 4. Repeated-load plate-bearing test apparatus.

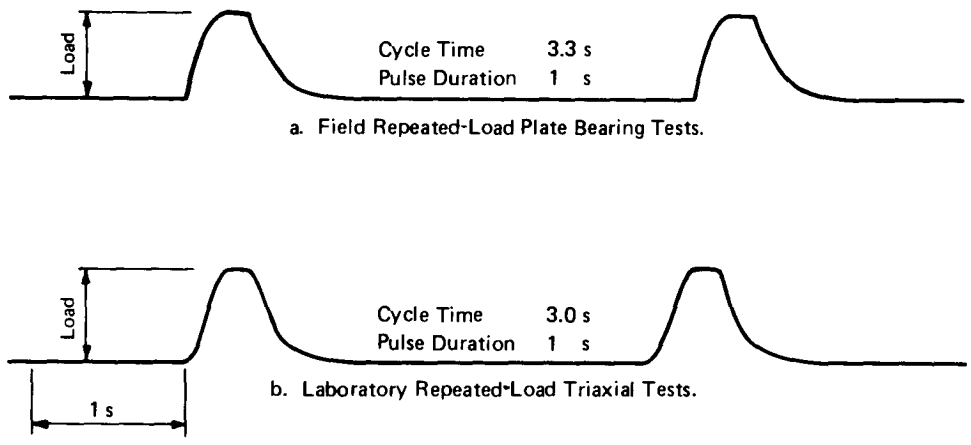

Figure 5. Load pulse waveforms.

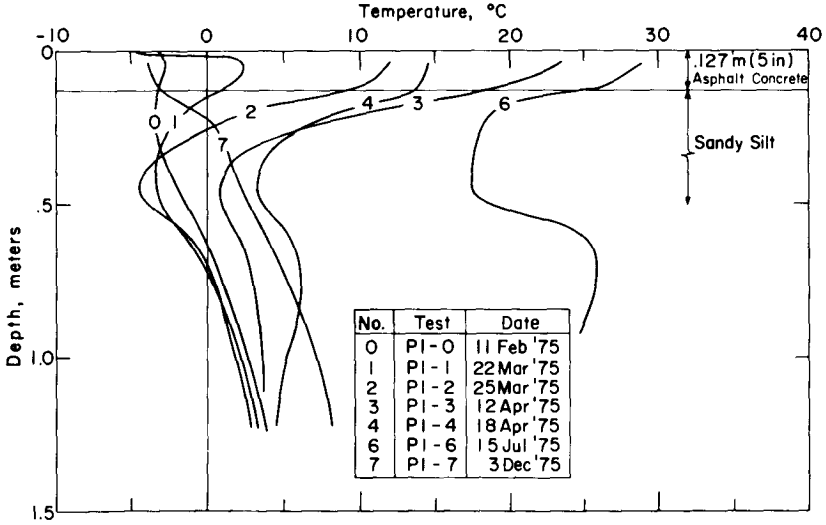

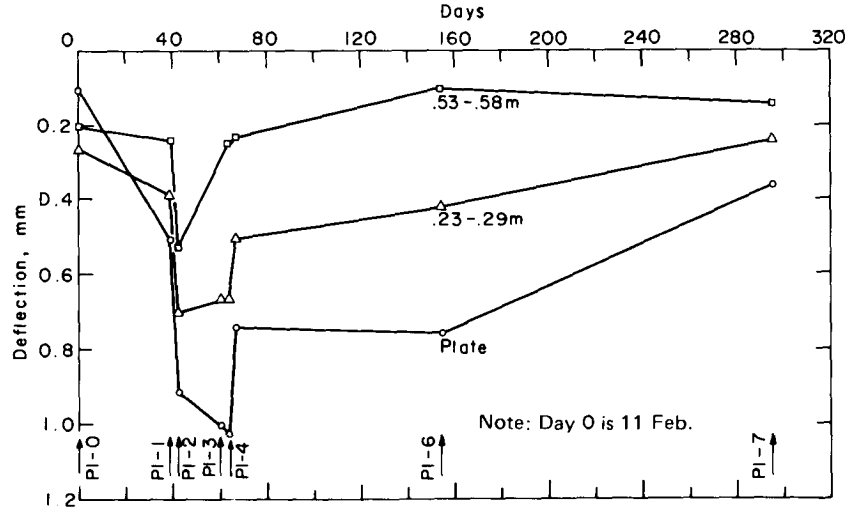

Test procedures and results

The equipment used in the tests is mounted on the back of a truck, the frame of which is supported on a heavy steel beam to provide a firm reaction for the plate load (Fig. 4). The load actuator works on adjustable air pressure, and loads up to about 53 kN can be applied at frequencies to about 20 per minute.

A load cell located on top of the plate produces a load signal for each load repetition, which is traced on strip charts by a pen recorder (Smith and Groves 1976). The resilient and residual deflections of the plate and of the pavement surface at various radial distances are measured with linear variable differential transformers (LVDT's), the outputs of which are traced by the same pen recorder. For the tests reported herein a load of about 40 kN was applied through a 304-mm-diam plate. The load was repeated 1000 times, with a waveform (Fig. 5a) that approximates slowly moving traffic.

Tests were performed at various stages in the annual cycle of freezing, thawing and strength recovery. Temperatures in the pavement and subgrade during the various tests (App. A) are typified by those shown in Figure 6, for test point P1.

The temperature tautochrones were drawn by interpolation between thermocouple data points spaced 38 to 76 mm apart in the upper 300 mm, and 150 to 300 mm apart to a depth of about 1.5 m. The most essential temperature data for analysis of deflections in the pavements are the temperature of the asphalt concrete, the depth of the 0°C isotherm(s) (which defines approximately the thickness of thawed and frozen layers in the subgrade), and the temperature of the frozen subgrade (Tables III and IV). For the analysis, the asphalt concrete for the 127-mm pavement was considered as one layer, while the 229-mm pavement was divided into two layers. The frozen silt was considered as one or two layers. Representative temperatures were determined for each layer from the thermocouple readings.

The observed resilient deflections for the series of tests at test point P1 are shown in Figure 7. Plotted deflections of the plate are the average of deflections at edge points separated by 90° of arc. It can be seen that there is an abrupt increase in deflection at about 40 days when thawing begins. The deflections at test point P1 show an equally abrupt decrease in deflection at about 65 days when the temperature of the asphalt concrete decreased, followed by a gradual recovery period of approximately 230 days, which ended when the subgrade started to freeze again. At other test points (App. A), the decrease occurred gradually, or a continued increase may be observed as the higher temperatures affected the asphalt concrete.

Table III. Pavement and subgrade temperatures, 0.127-m asphalt concrete pavement.

					Depth (m) below surface to bottom of:		Temperature (°C) of frozen soil			
	Date	Asph conc temp (°C)			Thawed	Frozen				
Test	1975	Surf	.127	0-.127	zone	zone	Layer		Layer	
P1-0	2/11	-3.0	-3.2	-3.2		.625	.127-.330	-3.3	.330-.625	-1.7
P1-1	3/22	-5.6	0.8	-2.2	.178	.711	.178-.330	-1.4	.330-.711	-2.2
P1-2	3/25	3.9	8.9	7.8	.254	.686	.254-.406	-1.9	.406-.686	-2.8
P1-3	4/12	16.1	19.2	18.9	complete					
P1-4	4/15	15.0	16.4	16.1	complete					
P1-5	4/18	5.6	13.9	11.7	complete					
P1-6	7/15	29.4	26.4	27.8	complete					
P1-7	12/3	-1.0	-3.3	-1.2		.203	.127-.203	-1.7		
P2-0	2/12	-9.0	-8.9	-8.9		.673	.127-.457	-5.6	.457-.673	-1.1
P2-1	3/18	6.4	8.9	7.8	.305	.635	.305-.635	-0.8		
P2-2	3/21	2.2	9.7	7.8	.305	.737	.305-.737	-1.1		
P2-3	4/18	3.9	12.2	27.8	complete					
P2-4	7/17	41.1	37.8	39.4	complete					
P2-5	12/4	5.8	-3.4	0.0		.178	.127-.178	-1.4		
P3-1	3/19	2.8	5.0	5.0	.254	.635	.254-.635	-0.8		
P3-2	3/21	-1.7	8.3	5.0	.305	.711	.305-.711	-1.1		
P3-3	4/12	11.1	18.0	16.7	complete					
P3-4	4/15	10.0	16.1	13.9	complete					
P3-5	4/18	5.0	13.3	10.6	complete					
P3-6	7/15	33.3	31.1	32.2	complete					
P3-7	12/3			0.6		.152	.127-.152	-1.1		

Table IV. Pavement and subgrade temperatures, 0.229-m asphalt concrete pavement.

Test	Date 1975	Asph conc temp (°C) Surf	.038	.229	0-.038	.038-.229	Depth (m) below surface to bottom of: Thawed zone	Frozen zone	Temperature (°C) of frozen soil Layer		Layer	
P4-0	2/13	-0.9	-2.4	-6.7	-1.7	-5.0		.737	.229-.381	-5.8	.381-.737	-2.2
P4-1	3/18	15.6	14.7	4.2	15.1	9.4	.305	.381	.305-.381	-0.3		
P4-2	3/25	8.6	8.3	3.6	8.4	6.1	.254	.457	.254-.457	-0.8		
P4-3	4/11	18.7	19.9	8.0	19.3	13.9	.584	.660	.584-.660	0.0		
P4-4	4/16	21.4	19.6	10.0	20.5	15.0	complete					
P4-5	4/18	16.7	16.9	12.2	16.8	15.0	complete					
P4-6	4/22	15.8	12.2	6.1	14.0	9.4	complete					
P4-7	7/16	23.6	21.4	26.4	22.5	23.9	complete					
P4-8	12/3	-0.2	-1.4	-1.2	-0.8	-1.7		.279	.229-.279	-0.6		
P5-0	3/4	2.6	2.4	0.1	2.5	1.1		.610	.229-.610	-0.6		
P5-1	3/18	5.3	6.7	4.7	5.9	6.1	.279	.406	.279-.406	-0.3		
P5-2	3/25	8.4	8.1	3.1	8.3	5.8	.254	.444	.254-.444	-1.1		
P5-3	4/12	6.1	6.1	3.9	6.1	5.3	complete					
P5-4	4/18	14.0	14.1	12.5	14.0	13.9	complete					
P5-5	7/17	31.4	28.0	26.0	29.7	27.2	complete					
P5-6	12/4	-2.8	-4.2	-4.2	-3.6	-4.2		.330	.229-.330	-1.7		
P6-1	3/19	7.2	7.2	3.2	7.2	5.8	.279	.406	.279-.406	-0.6		
P6-2	4/12	6.9	7.4	5.3	7.2	6.7	complete					
P6-3	7/16	29.7	27.6	26.8	28.6	27.2	complete					
P6-4	12/3	-0.8	-2.2	-1.9	-1.7	-2.2		.305	.229-.305	-1.1		

RESILIENT MODULUS OF SUBGRADE CALCULATED FROM FIELD TESTS

Mathematical model

To calculate the resilient modulus of the silt in the various stages of freeze-thaw cycling the pavement and subgrade were considered as an elastic layered system. Barenberg (1973) discussed some of the deficiencies of the layered system approach but concluded it is the best general mathematical model currently available for evaluating pavement systems. The model employed is that of Michelow (1963); the computer program was published by Warren and Dieckmann (1963). Kasianchuk (1968) modified the program to include an interaction technique that accounts for the dependency of the resilient moduli of bases and subgrade materials upon stresses.

Inputs to the computer program include the average vertical pressure applied by the plate, M_r and μ_r of asphalt concrete for the loading time and temperature of the test, and M_r and μ_r of all layers of the subgrade including trial values for the layer or layers for which the solution is desired. Program outputs include stresses, strains and displacements at various depths and radial distances.

Characterization of asphalt concrete

The stiffness moduli of asphalt concrete at various temperatures selected for use in the analyses are summarized in Figure 8, and the moduli corresponding to the temperatures prevailing during each test are summarized in Tables V and VI. Results of initial laboratory repeated-load triaxial tests (described below) at deviator stresses of 310 and 413 kPa were used as a guide in selecting moduli for surface courses, while the moduli for the binder courses for the 229-mm pavement were based on tests at 103 kPa. Tests on asphalt concrete from the 127-mm pavement were run only on composite samples, comprising the surface course and part of the binder courses. Hence, in the analysis of deflections also the modulus was assumed to be uniform throughout the 127-mm thickness. For the 229-mm pavement, on the other hand, composite samples of the surface and upper binder courses were tested and the results taken to represent the surface course, while the modulus of the binder courses was determined by tests on the lower layers of binder course material.

After the moduli were selected and used in the analyses of deflections measured in plate-bearing tests, additional laboratory testing of asphalt concrete was performed to evaluate the effects of moisture content;

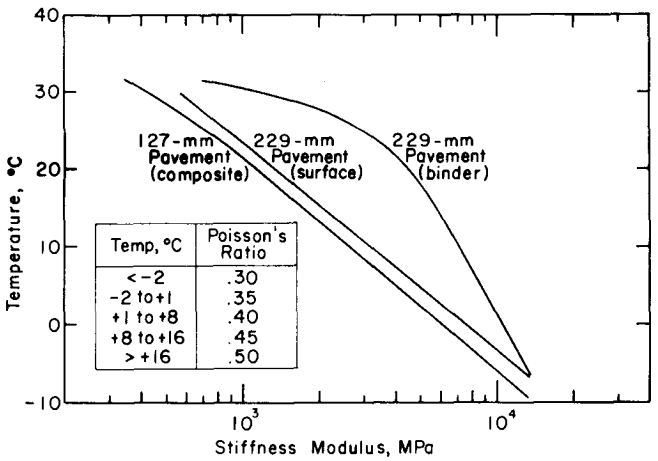

Figure 8. Stiffness modulus of asphalt concrete used in analysis.

Table V. Modulus of asphalt concrete and frozen silt, 0.127-m asphalt concrete pavement.

	Asphalt concrete, 0-0.127 m		*Thickness of thawed silt above frozen silt (m)*	*Thickness (m) and resilient modulus (GPa) of frozen silt*	
Test	*Stiffness modulus (GPa)*	*Poisson's ratio*		*Layer*	*Layer*
P1-0	7.93	.30		.203 8.96	.295 1.72
P1-1	7.58	.35	.051	.152 2.07	.381 4.14
P1-2	3.24	.40	.127	.152 3.31	.279 6.20
P1-3	1.27	.48			
P1-4	1.65	.47			
P1-5	2.34	.45			
P1-6	0.55	.49			
P1-7	7.58	.30		.076 2.62	
P2-0	13.10	.30		.330 17.9	.216 1.38
P2-1	3.24	.40	.178	.330 1.40	
P2-2	3.24	.40	.178	.432 1.72	
P2-3	2.76	.45			
P2-4	0.21	.50			
P2-5	6.20	.35		.051 2.07	
P3-1	4.00	.40	.127	.381 1.38	
P3-2	4.00	.40	.178	.406 1.72	
P3-3	1.59	.45			
P3-4	2.00	.45			
P3-5	2.62	.45			
P3-6	0.34	.50			
P3-7	5.86	.35		.025 1.52	

somewhat lower moduli were found for the moist asphalt concrete at temperatures above freezing (Fig. 18, page 20). The deflections were not re-analyzed using the later test data, in part because the somewhat lower moduli of the moist asphalt concrete in the higher temperature range have only a slight effect on the computed resilient moduli of the subgrade soil, and in part because it was decided to analyze the deflections also without predetermined moduli of asphalt concrete but instead with various lower trial moduli to seek better conformance of the deflection basins (see below).

Values of Poisson's ratio of the asphalt concrete, for use in analyzing the deflections, were selected based on review of published data (Sayegh 1967, Monismith and Secor 1962) and on the initial results from the laboratory

Table VI. Modulus of asphalt concrete and frozen silt, 0.229-m asphalt concrete pavement.

Test	Asphalt concrete: Stiffness modulus (GPa) 0-.038 m	Asphalt concrete: Stiffness modulus (GPa) .038-.229 m	Asphalt concrete: Poisson's ratio 0-.038 m	Asphalt concrete: Poisson's ratio .038-.229 m	Thickness of thawed silt above frozen silt (m)	Thickness (m) and resilient modulus (GPa) of frozen silt: Layer		Layer	
P4-0	8.96	12.76	.35	.28		.152	17.92	.356	2.76
P4-1	1.93	7.93	.45	.45	.076	.076	0.28		
P4-2	3.52	9.31	.45	.45	.025	.203	1.38		
P4-3	1.34	6.76	.45	.45	.356	.076	0.14		
P4-4	1.24	6.34	.50	.45					
P4-5	1.65	6.34	.50	.45					
P4-6	2.14	7.93	.45	.45					
P4-7	1.10	3.45	.50	.50					
P4-8	8.27	11.38	.35	.35		.050	1.17		
P5-0	6.21	10.00	.40	.40		.381	1.03		
P5-1	4.55	9.31	.40	.40	.050	.127	0.28		
P5-2	3.58	9.31	.40	.40	.025	.190	1.72		
P5-3	4.41	9.65	.40	.40					
P5-4	2.14	6.76	.45	.45					
P5-5	0.62	2.62	.50	.50					
P5-6	11.03	12.41	.30	.30		.101	2.62		
P6-1	4.00	9.31	.40	.40	.050	.127	1.17		
P6-2	4.00	8.96	.40	.40					
P6-3	0.67	2.62	.50	.50					
P6-4	8.96	11.72	.35	.35		.076	1.72		

testing described below. The values adopted for the analyses are shown in Figure 8 and Tables V and VI.

Characterization of frozen silt

During thawing and early stages of recovery, the pavement section still included a layer of frozen silt. The resilient moduli for the frozen silt (Fig. 9 and Tables V and VI) adopted for the analysis of plate-bearing tests to calculate the resilient molulus of the subgrade silt during thawing and recovery were taken from the initial results of laboratory tests summarized in Table BIV (App. B), and in particular from tests on sample HS-11-4 (Fig. 20) at values of σ_3 from 69 to 103 kPa. Later laboratory tests showed somewhat lower values at moisture contents more representative of in-situ conditions. The plate-bearing tests were not re-analyzed using these somewhat lower values for frozen silt because it is believed that the latter would have only a moderate effect on the calculated moduli of the overlying thawing or thawed silt. As values for μ_r for the frozen silt were not obtained in the laboratory test program, a value of 0.26 was selected from Stevens' (1975) tests, determined from vibratory (1 kHz) loading of Manchester silt at –3.9°C.

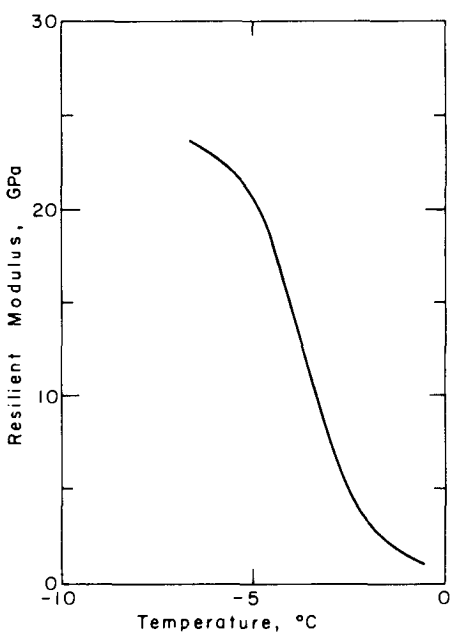

Figure 9. Resilient modulus of frozen silt used in analysis.

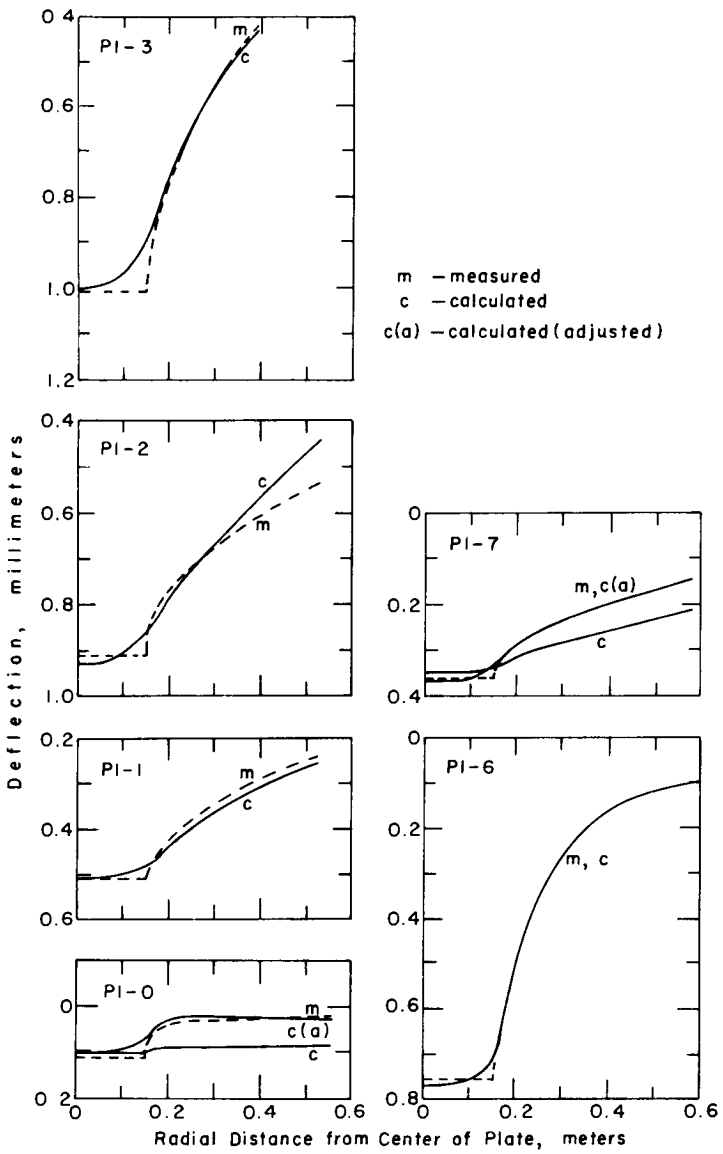

Figure 10. Measured and calculated deflection basins, test point P1.

Calculated resilient modulus of silt within the zone of freezing

The deflection basins measured in six tests at test point P1 are shown in Figure 10; the dates of the tests and the temperatures prevailing at the time of each test are shown in Figure 6. By solving for the surface deflections given by the layered elastic theory for successive trial resilient moduli of the thawing or recovering silt layer, the modulus that gave the best fit with the observed plate deflection was found; the resulting calculated deflection basins also are shown in Figure 10.

In many cases the entire calculated deflection basin coincided acceptably with the observed basin, as for example P1-1, P1-3 and P1-6. In other cases (P1-0 and P1-7) the deflection basins differed markedly, and only by using substantially lower moduli for the asphalt concrete could the deflection basins be made to coincide. At the other test points on the 127-mm pavement, P2 and P3, the degree of coincidence of calculated and observed deflection basins (Fig. A6, App. A) was about the same as at P1. The divergence was much greater at test points on the 229-mm pavements, P4 (Fig. 11), P5 and P6 (Fig. A5, App. A). At P4, for example, all tests showed a much more effective damping of surface deflections at increasing radial distances, compared with the deflection basins calculated from the elastic layered system analysis using as an input the asphalt

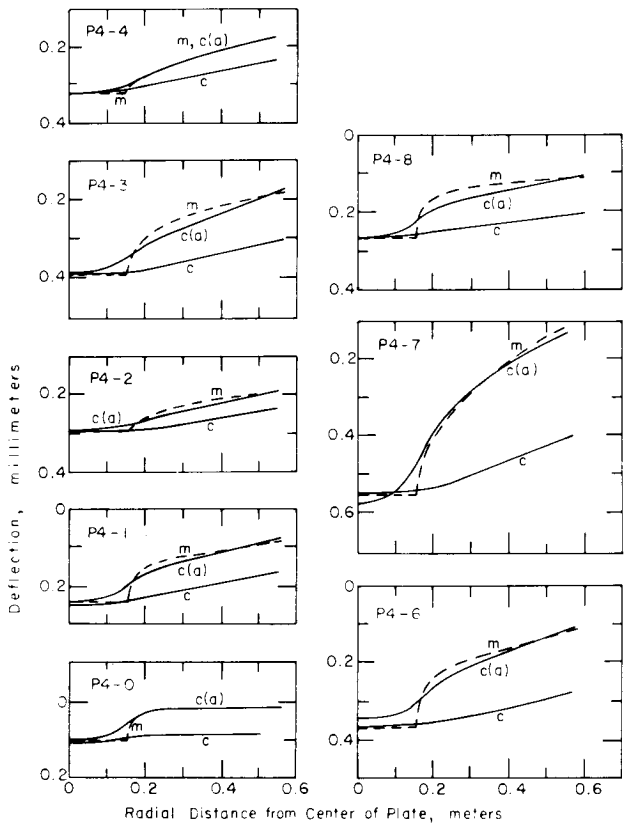

Figure 11. Measured and calculated deflection basins, test point P4.

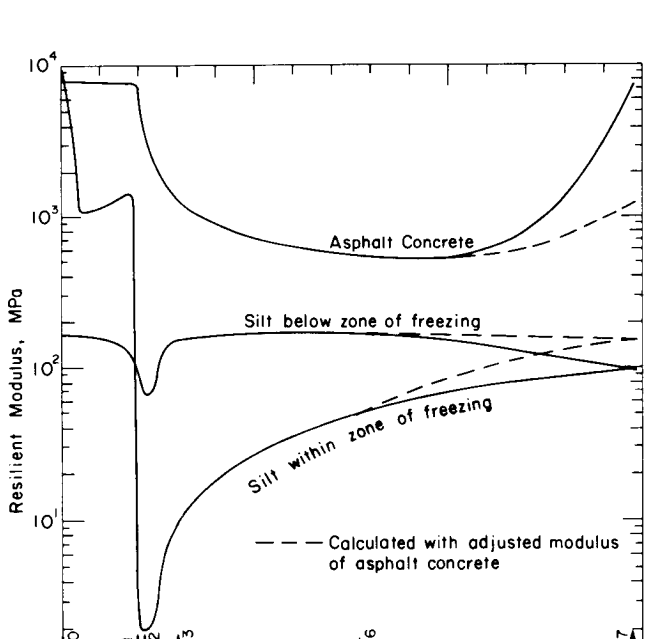

a. Test point P1.

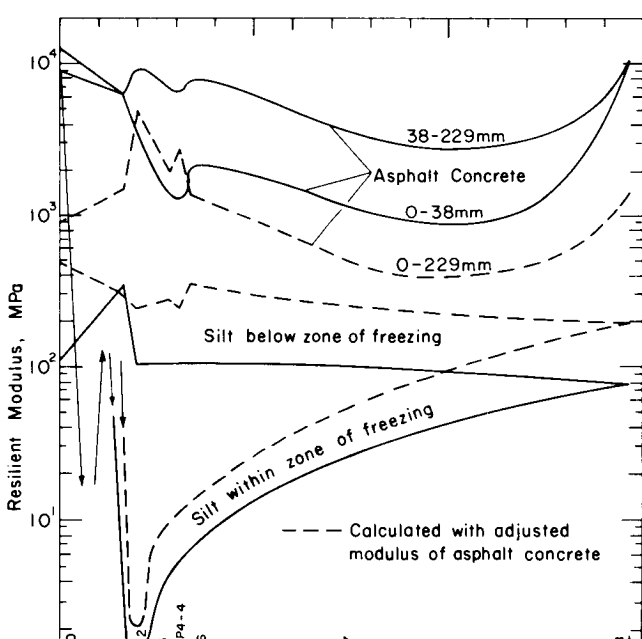

b. Test point P4.

Figure 12. Calculated resilient moduli of subgrade silt, and moduli of asphalt concrete used in analyses, test points P1 and P

concrete moduli summarized in Figure 8. By using substantially lower trial moduli of asphalt concrete (Fig. 12b), compensated with higher trial moduli of silt within and below the zone of freezing to yield a calculated plate deflection equal to the observed, it was found the deflection basins could be made to coincide closely (Fig. 11).

It does not seem implausible that the problem of nonconformance of the deflection basins is indeed attributable to the asphalt concrete, because later tests on moist asphalt concrete showed somewhat lower moduli, because the asphalt pavement responds to surface loads in a flexural mode for which moduli lower than the compression moduli actually used might apply, and because the discrepancy is encountered more frequently and is more pronounced in those cases in which an error in assessing the modulus of the asphalt concrete would have the greatest impact on the results. Those cases include the frozen condition, when the asphalt concrete sometimes is no stiffer than the silt; certain of the summer-fall tests when the modulus of the asphalt concrete is decreased by high temperatures; and the tests on the 229-mm pavement, for which the asphalt concrete, being thicker, has a more dominant influence on the surface deflection. It is recognized, however, that part of the discrepancy could be attributable to inappropriateness of an elastic layered system model, compared with the undoubtedly inelastic behavior of the materials. The rigidity of the loading plate also limits the applicability of the model, which assumes uniform stress distribution beneath the plate. Nevertheless, it is believed the possible inaccuracies deriving from use of an elastic model will be compensated in part by the use of the same model for design, calculating stresses and strains based upon inputs that include those same moduli. Consequently, and in spite of the uncertainties mentioned above, it is believed the calculated moduli of the silt, which are simply those trial values giving the best fit of the resilient movements of the plate and the deflection basins, are not grossly inaccurate, and represent reasonably well the moduli applicable for use in design.

The calculated moduli of the subgrade silt at test points P1 and P4 are shown in Figure 12, together with the asphalt concrete moduli on which each of the calculations was based. The date of each test is given in Figure 6. The corresponding data for test points P2, P3, P5 and P6 are given in Figure A7 (App. A). The moduli for asphalt concrete shown as solid lines in Figure 12 are taken from test data summarized in Figure 8, while the dashed lines for the asphalt concrete are those trial values that, with various trial values for the silt within the zone that had been frozen earlier, give the best fit of the deflection basins. The moduli for silt within and below the zone of freezing shown in solid lines were determined as the trial values giving the best fit of the deflections basins with test values for the asphalt concrete, while the dashed lines are the results using the lower, adjusted, asphalt concrete moduli.

For each calculation, input parameters included not only trial moduli but layer thickness. For asphalt concrete, thicknesses were measured and known. The silt below the zone of freezing was in each case assumed to be semi-infinite in extent. For frozen silt, actual thickness determined from thermocouple data (Tables III and IV) were used for the calculations. The thickness of the weakened layer of thawed silt, however, was varied somewhat. When partial thawing had occurred, the actual thickness of thawed silt existing above frozen silt was used. When the silt became fully thawed, however, the choice of layer thickness became an object of trials in the quest for the best fit of deflection basins, just as the moduli also were entered as trial values. Thickness of thawed silt was in each case either equal to or less than the thickness of silt that had been previously frozen. In many cases a better fit of deflection basins was found, with a thickness of weakened thawed silt somewhat less than the previously frozen thickness (Table VII), possibly indicating nearly complete recovery in the lower part of the thawed silt.

It is not known whether the calculated resilient moduli of subgrade silt that result from analyses based on adjusted asphalt concrete moduli, which give coincident calculated and observed deflection basins, are more accurate than those based on coincident deflections only at the plate. For tests on the 127-mm pavement, while the subgrade is weakened by thaw, the differences in the calculated moduli are not significant and it appears unnecessary to seek coincidence of the entire deflection basins. For tests on the 229-mm pavement, however, the differences are significant (Fig. 12b). Furthermore, at test points P5 and P6 (Fig. A7, App. A), the calculated moduli, whether based on coincidence of plate deflection only or the entire deflection basins, seem to change with time in a rather irregular manner (Table VIII). Results of tests on the 127-mm pavement, on the other hand, are reasonably consistent, and the recovery proceeds in a regular way with time, thereby inspiring greater confidence in the validity of the calculated moduli.

The vertical compressive strains within the thawing silt caused by plate loading are, of course, much higher beneath the 127-mm pavement, exceeding by nearly one order of magnitude those beneath the 229-mm pavement. This difference is consistent with an expectation that the thicker pavement would perform

Table VII. Layer thicknesses H* and trial resilient moduli M_r† of silt within zone of freezing giving best fit of deflection basins.

	Before thaw		Partial thaw						Complete thaw								
		Frozen soil	Thawed soil			Thawed soil			Weakened soil			Weakened soil			Weakened soil		
Test point	Test	H	Test	Mr	H	Test	Mr	H	Test	Mr	H	Test	Mr	H	Test	Mr	H
P1	1-0	50	1-1	3.4	5	1-2	2.1	13	1-3	10.3 17.3	15 15	1-6	51.7	25			
P2	2-0	55	2-2	4.5	18				2-3	13.8	30	2-4	55.1	30			
P3		(51)	3-1	2.8	13				3-3	3.8 27.6	15 15	3-5	5.5	15	3-6	44.8	15
P4	4-0	51	4-2	1.4	5	4-3	5.5	36	4-4	19.3	30	4-6	6.2	30	4-7	2.8	30
P5	5-0	38	5-2	0.7	5				5-3	2.2	20	5-4	1.6	30	5-5	3.2	30
P6		(38)	6-1	4.1	5				6-2	1.0	18	6-3	2.8	25			

* Thicknesses expressed in mm.
† Resilient moduli expressed in MPa.

Table VIII. Resilient moduli M_r* of silt during thawing and recovery.
Values in parentheses calculated with reduced moduli of asphalt concrete, giving deflection basins similar to observed basins.

Test point	Min Mr at thaw (MPa)	Mr, MPa, at indicated days after minimum			
		20	60	100	260 ± (terminal)
P1	2.1	11.4	27.6	45.5	96.6 (151.7)
P2	4.4	9.7	26.9	45.5	103.5 (137.9)
P3	2.6 (5.5)	4.1 (6.9)	17.3 (19.3)	37.3 (24.2)	89.7 (137.9)
P4	1.4 (2.1)	5.1 (10.4)	13.1 (25.5)	22.1 (48.3)	76.0 (193.0)
P5	0.7 (2.8)	1.4 (27.6)	2.2 (27.6)	2.9 (22.1)	55.1 (213.7)
P6	1.0 (137.9)	1.2 (96.7)	1.9 (27.6)	3.2 (13.8)	103.5 (206.8)

* Values taken from plots of calculated Mr, Fig. 12 and Appendix A.

acceptably under a much greater number of repetitions of a given wheel load, than the 127-mm pavement. The greater consistency of the test results from the latter pavement suggests that tests of this type should preferably be conducted on pavements designed to withstand a modest number of repetitions (perhaps no more than a few tens of thousands) of a wheel load that produces strains comparable to those produced by the plate load.

LABORATORY REPEATED-LOAD TRIAXIAL TESTS

Specimens, equipment and testing procedures

As repeated-load plate-bearing test data for a given subgrade soil will seldom be available for use in designing new pavements, it is convenient to employ laboratory tests to characterize the stress-deformation response of soil affected by freezing and thawing. To develop suitable techniques for this purpose, laboratory repeated-load triaxial tests were performed on asphalt concrete and silt cores 50 mm in diameter, taken from the pavement test sections. Asphalt concrete cores were tested under varying temperatures, moisture conditions and deviator stress levels. The silt specimens, taken from the test pavements in the frozen condition, were tested at several subfreezing temperatures as well as in the thawed condition for a range of deviator stresses and moisture contents. Undisturbed samples also were taken in the fall, and tested at in-situ moisture content and density to represent the fully recovered condition.

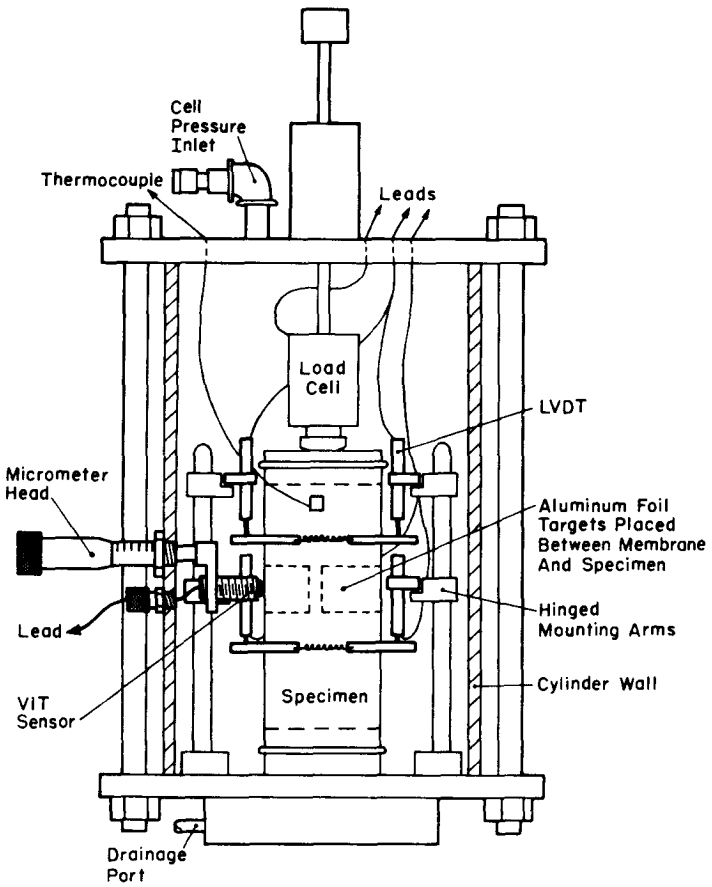

Figure 13. Triaxial cell.

Apparatus

The test specimens were mounted in the triaxial cell as seen in Figure 13. Axial deformation measurements were obtained using four LVDT's. The stems were mounted on spring-loaded Plexiglas clamps at third points on the sample. The barrels were individually mounted on arms with two hinged joints to allow freedom of movement in the horizontal plane.

Direct radial deformation measurement was made with three noncontacting variable impedance transducers (VIT's) equally spaced about the specimen at mid-height and mounted on the triaxial cell cylinder. Each transducer required an aluminum foil target placed between the specimen and the rubber triaxial membrane.

A miniature load cell mounted inside the triaxial cell served as a monitor for the axial load and a feedback source for the testing machine. The load cell output, the sum of the three VIT outputs, and the average of the LVDT outputs were recorded simultaneously on a high-speed pressurized-ink strip-chart recorder. Typical sets of load and deformation outputs for silt and asphalt concrete are shown in Figure 14.

The cyclic load was applied by a closed-loop electrohydraulic testing machine (see App. D). An electromechanical device was programmed to produce the load pulse waveform (see Fig. 5b). The pulse duration was 1 second and frequency 1 cycle per 3 s. Test temperatures were monitored by a digital thermometer. Compressed nitrogen was used as the cell fluid.

Procedures

The asphalt concrete cores were trimmed to length (approximately 127 mm), and the ends and sides ground smooth with a high-speed grinder mounted on a lathe carriage. Specimens were subjected to a test series in their original (air-dried) condition and certain of the specimens were retested after being subjected to the following saturation procedure. A 95-kPa vacuum was applied for about two hours. The chamber was then flooded with deaired, distilled water and remained

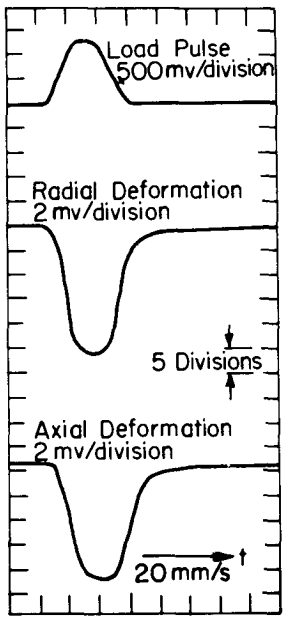

Typical Stripchart Recording
FD-5-2 σ_3=27.6 kPa, σ_d=13.8 kPa

a.

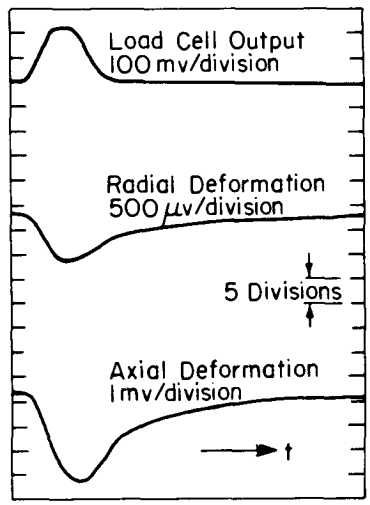

FD-9-2A, T=33.1 °C
σ_3=103.4 kPa, σ_d=103.4 kPa

b.

Figure 14. Typical load and deformation strip-chart recordings.

Table IX. Stress levels and testing sequence for triaxial tests on silt.

Confining stress σ_3 *(kPa)*	*Deviator stress** σ_d *(kPa)*	*Axial stress* σ_1 *(kPa)*	*Stress ratio** σ_1/σ_3	*Confining stress* σ_3 *(kPa)*	*Deviator stress** σ_d *(kPa)*	*Axial stress* σ_1 *(kPa)*	*Stress ratio** σ_1/σ_3
Frozen silt†				**Thawed silt (cont'd)**			
69	69	138.0	2	69	34.5	103.5	1.5
	137.9	206.9	3		69	138.0	2
	206.9	275.9	4		103.4	172.4	2.5
	344.8	413.8	6		137.9	206.9	3
	413.7	482.7	7	103.4	51.7	155.1	1.5
	551.6	620.6	9		103.4	206.8	2
					155.1	258.5	2.5
Thawed silt				**Recovered silt**			
6.9	3.4	10.3	1.5				
	6.9	13.8	2	13.8	26.9	40.7	3
	10.3	17.2	2.5	27.6	55.2	82.8	3
	13.8	20.7	3	69.0	135.1	204.1	3
	20.7	27.6	4	137.9	268.2	406.1	3
27.6	13.8	41.4	1.5	6.9	20.7	27.6	4
	27.6	55.2	2	13.8	44.8	58.6	4
	41.4	69	2.5	27.6	83.4	110.0	4
	55.2	82.2	3	69	203.4	272.4	4
	82.7	110.3	4	137.9	388.9	526.8	4

* Actual deviator stress levels, and therefore the stress ratio, varied somewhat from the intended values given here.
† Stress levels for sample HS-11-4 varied from those given here. See Table BIV (App. B).

under the vacuum for another two hours. Then the specimen was removed, blotted to remove excess surface moisture, and tested. A final test series was performed after specimens were dried in a desiccator. Resulting moisture contents ranged from 0 to 2%. Test temperatures ranged from −6.7°C to 32.2°C. Stress condition was not considered to be a major independent variable for this investigation, and the minor principal stress was 103.4 kPa for all tests. Deviator stress levels were 103.4 kPa for the 32.2°C tests, and 206.8 kPa for all others. Load was applied for 200 cycles, or until a stable response was obtained.

The silt cores were cut to length on a band saw while frozen. Ends were trimmed flat using a lathe. Tests on frozen specimens were conducted at several temperatures from −6.7°C to −0.8°C. It was desired to assess the effect of a broad range of stress conditions corresponding to those experienced under actual traffic loading, and deviator stress levels from 69 kPa to about 660 kPa were employed in the tests. Confining pressure was 69 kPa for all tests on frozen specimens. Specimens were thawed and consolidated to varying degrees to obtain a range in sample properties. Tests on thawed specimens were at room temperature (22.2°C). The deviator stress ranged from 3.5 kPa to a high of 172.4 kPa, while the confining pressures ranged from 6.9 kPa to 103.4 kPa. These stress levels were selected to conform with the range of vertical and tangential stress levels that might be developed in the silt during plate-bearing tests. The stress conditions of triaxial tests on frozen and thawed silt are summarized in Table IX.

RESILIENT PROPERTIES CALCULATED FROM LABORATORY TESTS

Calculation methods

The resilient modulus M_r was calculated as the ratio of the repeated deviator stress σ_d to recoverable axial strain ϵ_a. The resilient Poisson's ratio μ_r was calculated as the ratio of the recoverable radial strain ϵ_r to the recoverable axial strain ϵ_a. The M_r and μ_r values obtained in this way are secant values rather than the slopes of the tangents to the stress/axial strain and radial strain/axial strain curves. Calculation of secant values is a generally accepted method of determining resilient parameters (Allen and Thompson 1974).

The calculated resilient parameters were analyzed using multiple linear regression and analysis of variance techniques to obtain empirical relationships between M_r and μ_r, respectively, and the most significant variables. Correlations were found with various functions of the principal and deviator stresses, with the material parameters moisture content w and dry density γ_d, and, for asphalt concrete and frozen silt, with temperature. Models were selected to represent behavioral rather than mechanistic characteristics in order to obtain relatively simple relationships. The purpose of obtaining the models was to gain access to M_r and μ_r for a wide range of conditions. The analysis of variance techniques allowed the selection of the variables to be based on an acceptable significance level. All variables passed an F-test significance level (Gibra 1973) of 0.05. The multiple linear regression analysis yielded regression coefficients, correlation coefficients and standard errors for the various parameters passing the F-test. Equations most accurately fitting the laboratory data were selected based on the correlation coefficients and standard errors.

Asphalt concrete — test results

The results of all repeated-load triaxial tests on asphalt concrete cores are presented in Tables BI, BII, and BIII (App. B), including calculated values of resilient modulus and Poisson's ratio. Resilient moduli for two specimens, each at three levels of moisture content, are plotted for a range in temperatures in Figure 15. Resilient moduli for the same two specimens and two others are plotted for a range in moisture contents in Figure 16. The resilient modulus M_r for the asphalt concrete is observed to be primarily a function of temperature, decreasing by almost two orders of magnitude between −5°C and 30°C. Test specimens at temperatures higher than 0°C generally exhibited a decrease in resilient strain with decreasing moisture content, while the reverse was true for temperatures below 0°C.

Schmidt (1974) found that moist asphalt concrete does not show a smooth transition in the resilient characteristics as the temperature passes through the freezing point. In the same work, Schmidt found that the presence of moisture does not significantly affect the temperature susceptibility of hot asphalt-treated mixes. These two conclusions provide the basis for the form of the plots of M_r versus temperature (Fig. 15), which include discontinuities at 0°C. It must be noted that most test specimens suffered permanent damage to varying degrees from vacuum saturation and subsequent testing (see Fig. 17). The effect this had on the resilient response of the specimen in later tests, if significant, is difficult to determine. Specimen damage was of both the cohesive type [cracking indicating failure in the asphaltic binder (Fig. 17a)] and the adhesive type [failure of the binder-aggregate bond (Fig. 17b)].

The initial test series on asphalt concrete specimens (Table BIII, App. B) was performed prior to the

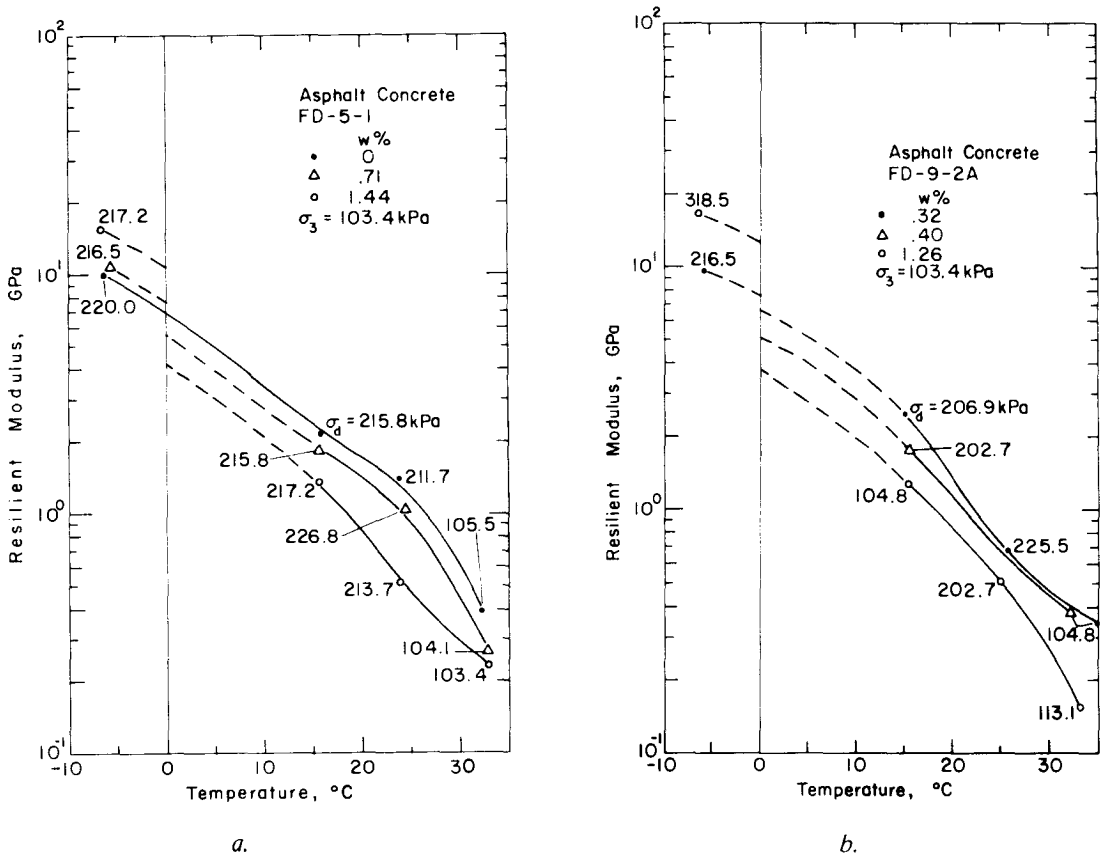

a. *b.*

Figure 15. Effect of temperature on resilient modulus of two asphalt concrete specimens.

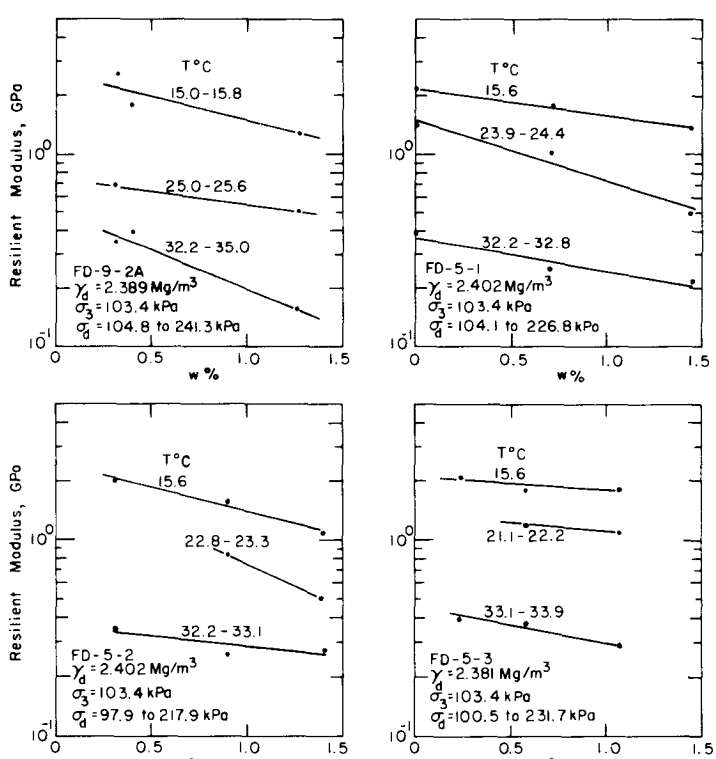

Figure 16. Effect of moisture content on resilient modulus of four asphalt concrete specimens.

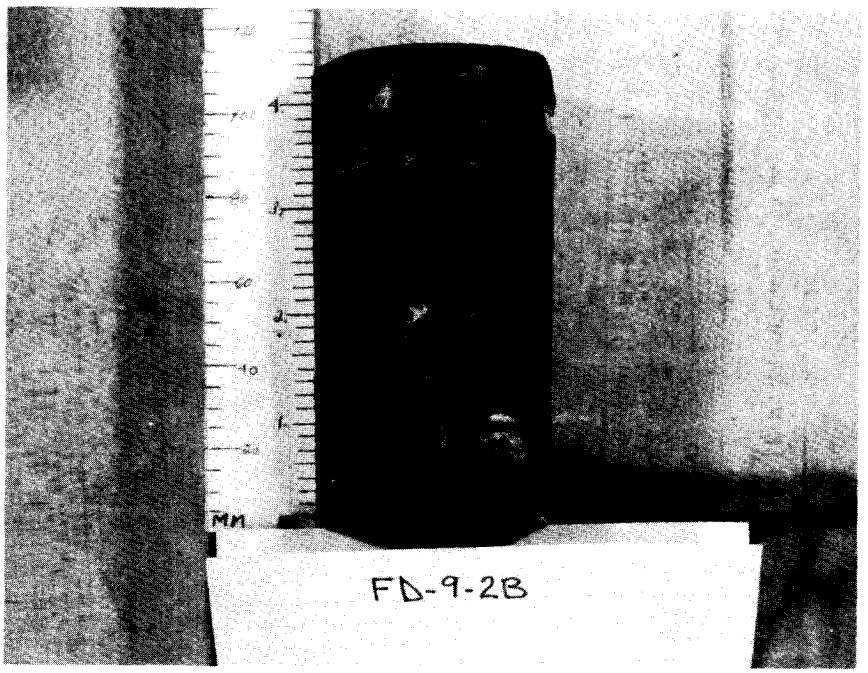

a.

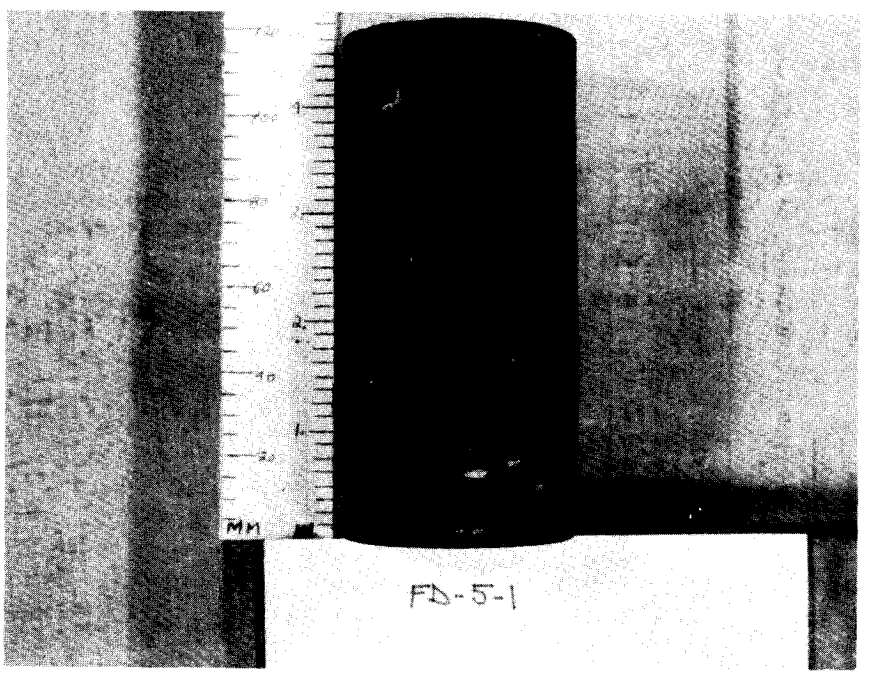

b.

Figure 17. Asphalt concrete specimens after testing for moisture-induced damage.

development of the radial deformation measurement system. Thus, no information on Poisson's ratio is available for these specimens. Also, the axial deformation measurement system was in developmental stages at that time. Thus, there is an increased probability that the inconsistencies in these data are a result of inadequate response in the deformation measurement system. Nonetheless, the strong influence of temperature on M_r is apparent. The decrease in M_r of about two orders of magnitude, over a range in temperatures from –6.7°C to 32.2°C, is consistent with results presented for the later tests (Table BII, App. B).

Values of Poisson's ratio μ_r in excess of 0.5 as well as inordinately low values were calculated in several instances. Non-uniform radial deformations at the sensor locations appear to be the cause of these extraneous values. The average values for μ_r were 0.33, 0.39, and 0.40, for test temperatures of 15.6, 23.9, and 32.2°C, respectively. This range of values and the tendency of μ_r to increase with increasing temperature are consistent with values reported by Nair and Chang (1973), Schmidt and Graf (1972) and Pell and Brown (1972a and 1972b). Values for μ_r at negative temperatures could not be calculated because the radial strains were generally too small to record.

Asphalt concrete – statistical analysis and discussion

Results of tests on frozen and thawed specimens were analyzed separately, since the data did not adequately characterize the –5°C to +15°C range. For tests on frozen specimens, the small range in subfreezing temperatures precludes the development of an empirical relationship containing a temperature variable. However, an expression was developed using the least squares analysis technique relating M_r to moisture content, with other parameters assumed constant:

$$M_r\,(\text{MPa}) = 1.014 \times 10^4 + 2.51 \times 10^3\, w$$

where w is moisture content in percent. This expression is valid for $0 \leq w \leq 2\%$.

Test results on specimens at temperatures above 0°C were analyzed by multiple regression techniques. Equations were developed using both M_r and ln M_r as the dependent variables (App. C). The strongest multiple correlation coefficient ($R^2 = 0.91$) was obtained in the equation with ln M_r as the dependent variable:

$$\ln M_r = 16.467 - w(.4064) + \sigma_d\,(2.293 \times 10^{-3}) - T(.1797) + T^2\,(1.856 \times 10^{-3})$$

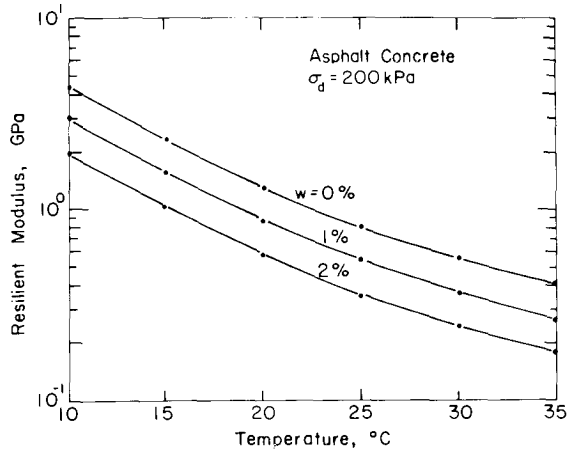

Figure 18. Results of regression analysis, effect of temperature and moisture content on unfrozen asphalt concrete.

where M_r and σ_d are expressed in kPa, T in °C and w in percent. The range of validity of the expression is $15°C \leq T \leq 35°C$, 100 kPa $\leq \sigma_d \leq$ 225 kPa and $0 \leq w \leq 2.0\%$. Figure 18 shows the resilient moduli given by this equation for a range of temperatures and moisture contents at a deviator stress level of 200 kPa.

The sign of the coefficient of σ_d differs from the usual pattern of decreases in M_r with increases in σ_d. This apparent reversal comes about only because σ_d was lowered for the high temperature tests to prevent excessive specimen damage. But in the statistical analysis the net result appears as a decrease in M_r, being caused, in part, by the decrease in deviator stress as well as the increase in temperature. Consequently this equation, which primarily examines the effect of w and T on M_r, should be used only with relatively low values of σ_d within the range of the test parameters.

Although there are some noticeable inconsistencies in the test data, the statistical analysis shows that on the whole M_r decreased by more than 30% for each percent increase in moisture content at 25°C. According to the rather limited least squares analysis, M_r increased by approximately 25% for each percent increase in moisture content at –5°C. M_r also decreased by as much as 35% for an increase in deviator stress from 103.4 kPa to 310.3 kPa, according to tests in the air-dry condition summarized in Table BIII (App. B). Confining stress level had little effect on M_r.

Schmidt and Graf (1972) and Schmidt (1974) have shown that the rate and extent of the change in M_r induced by the presence of moisture are, in part, a function of the material characteristics of the asphalt concrete, the length of soaking time after vacuum

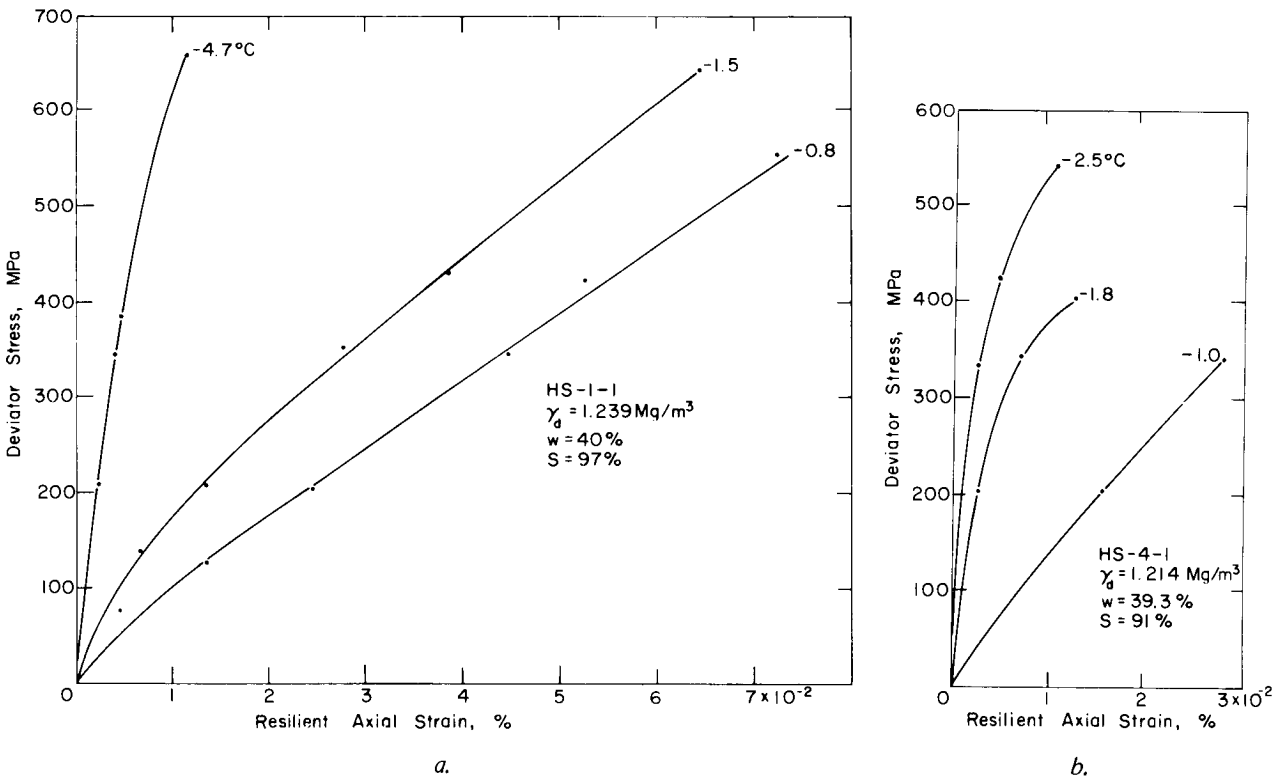

Figure 19. Resilient axial strains and deviator stresses measured on two specimens of frozen silt.

saturation, and freeze-thaw history. The inevitable variations in the specimen characteristics of the field cores used here would account in part for the range in the observed detrimental effects of moisture.

An in-depth study of the effects of moisture on the asphalt concrete was not within the scope of this work. However, it was desired to establish the general trend in this regard, but without inducing excessive damage to the specimens, as this would affect subsequent testing. Thus, a relatively short soaking time of two hours was used, representing a moderate but realistic degree of moisture-induced damage. (Schmidt [1974] has suggested a soaking period of seven days at 22.8°C after vacuum saturation to determine the maximum amount of moisture-induced damage.)

Although the average test values of Poisson's ratio given above show a consistent increase with temperature, the data exhibited excessive scatter, and consequently did not respond well to statistical analysis for correlation with material and test parameters.

Silt – test results

The results of all repeated-load triaxial tests on specimens of silt are presented in Appendix B. Included also are calculated values of resilient modulus for frozen, thawed, and fully recovered silt. Radial strains and calculated values of Poisson's ratio are given for the thawed silt. Poisson's ratio could not be determined for the frozen silt because radial strains were generally too small to measure accurately.

Deviator stresses are plotted against resilient axial strain for two frozen specimens in Figure 19, for a range in subfreezing temperatures. Figure 20 shows stress-strain curves for a third frozen specimen, as well as the corresponding plot of resilient modulus against temperature. The resilient modulus is observed to decrease more than one order of magnitude as the temperature approaches the melting point, ranging from over 1×10^4 MPa at –6.5°C to less than 1×10^3 MPa at –0.5°C. The influence of σ_d on M_r varies with temperature, being poorly defined to moderate at –4 to –6.5°C, while at higher subfreezing temperatures a 100% increase in σ_d results in a decrease of about 30 to 80% in M_r (Table BIV, App. B). The parameters σ_3, w, and γ_d did not appear to affect significantly the results for the range of conditions imposed. All test data for frozen silt are given in Table BIV (App. B).

Upon thawing, most samples were too soft and weak to test, and had to be either partially or fully consolidated before applying the repeated load. The different degrees of consolidation are reflected in differing moisture contents of the various specimens, which range from about 31 to 39%. The results of all

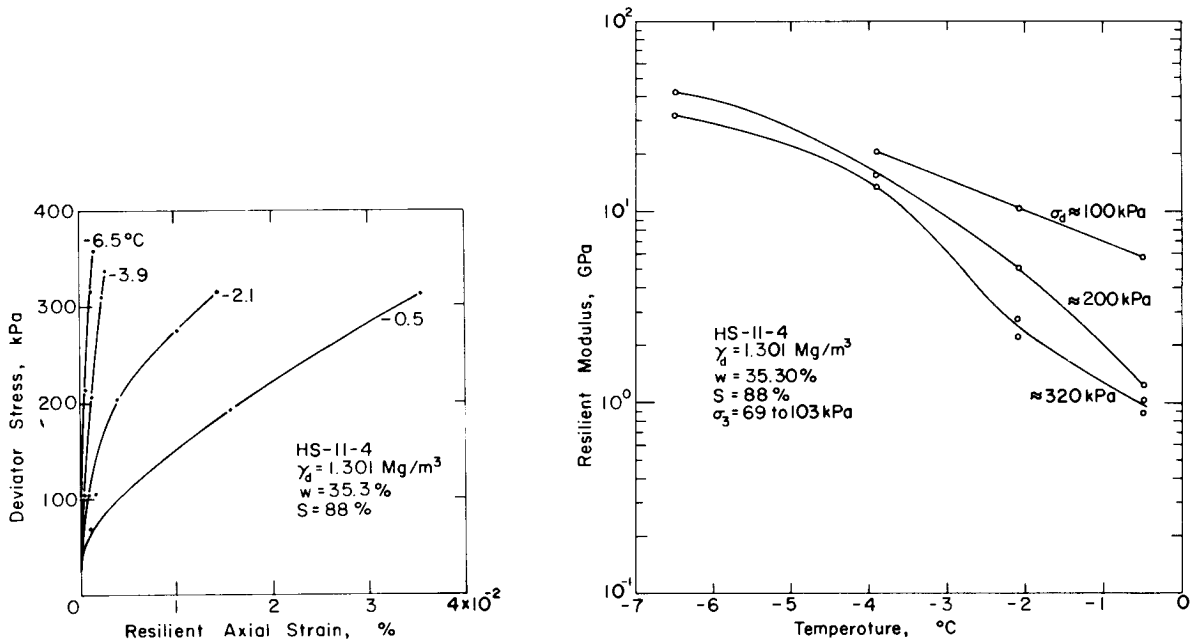

a. *b.*

Figure 20. Resilient axial strains and resilient moduli determined on frozen silt specimen HS-11-4.

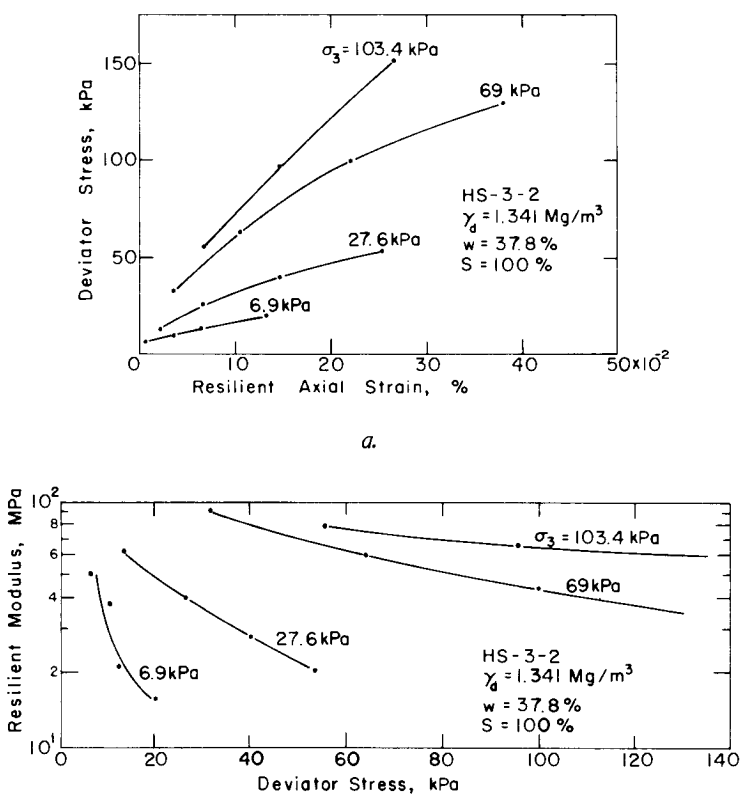

a.

b.

Figure 21. Resilient axial strains and resilient moduli, thawed silt specimen HS-3-2.

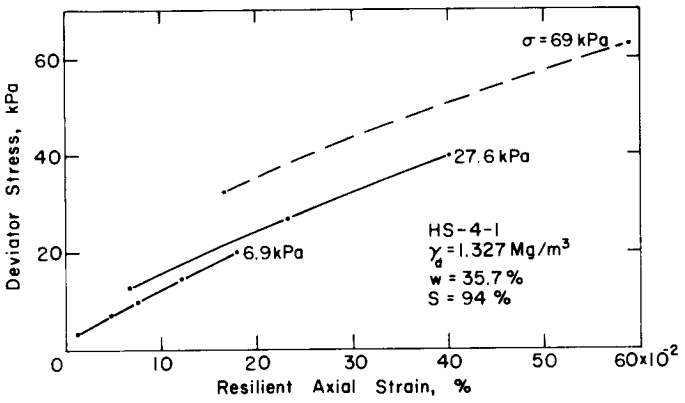

a.

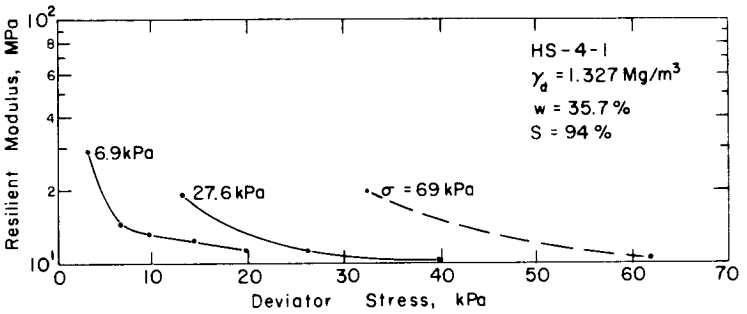

b.

Figure 22. Resilient axial strains and resilient moduli, thawed silt specimen HS-4-1.

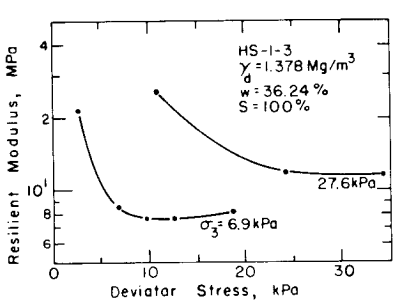

a.

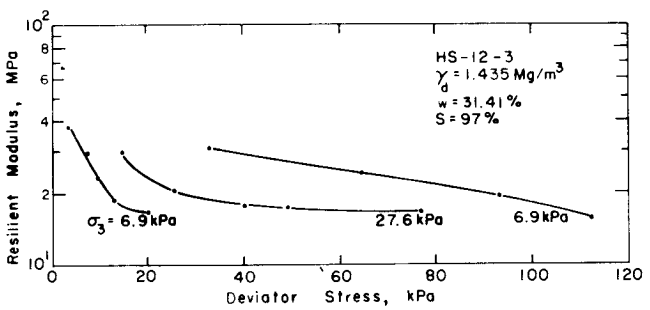

b.

Figure 23. Resilient moduli of two thawed silt specimens.

repeated-load triaxial tests on thawed silt are shown in Table BV (App. B), including calculated values of resilient modulus M_r and Poisson's ratio μ_r. Deviator stresses are plotted against resilient axial strain for two specimens in Figures 21 and 22. Resilient moduli are also plotted against deviator stresses for the same two specimens in Figures 21 and 22, and for two other specimens in Figure 23.

The data for thawed specimens show that increasing the deviator stress decreased M_r significantly (the greatest decrease occurring at the lower moisture contents), while increasing confining pressure and dry density increased M_r. While not shown clearly by the test data, the statistical analysis (see below) shows that the most significant factor affecting M_r was moisture content, with M_r increasing by factors of seven to eight as w decreased from 40% to 32% (see Fig. 27).

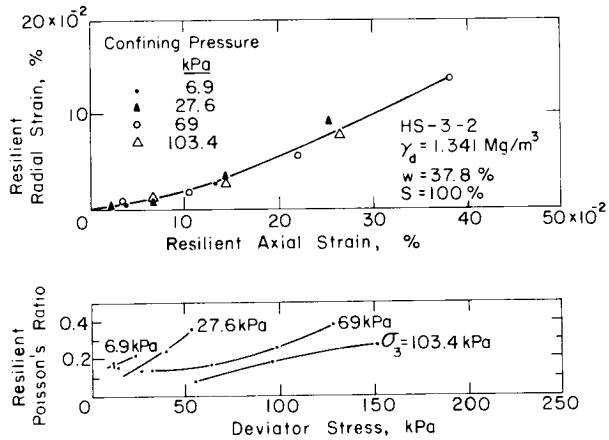

a.

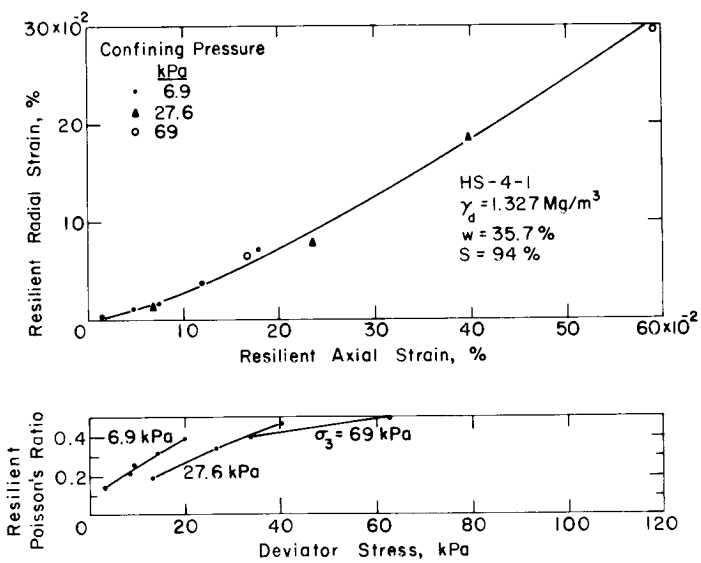

b.

Figure 24. Resilient radial strains and Poisson's ratio for two thawed silt specimens.

With the two specimens having the highest moisture contents, HS-1-1 and HS-3-1, the resilient modulus increased as load cycling progressed through the test series at increasing levels of deviator stress and confining pressure (Table BV, App. B), reversing the pattern observed in the majority of the specimens, for which M_r decreased as the deviator stress increased. The reason for the anomalous behavior of the two specimens is not known. Possibly it may be a manifestation of progressive recovery from the weakened state.

Shackel (1973) attributed decreases in resilient strains during load cycling on unfrozen soil specimens to complex alterations in the soil structure as well as increases in density. The gradual redistribution of water which existed as segregated ice in the specimens tested here, resulting in a more uniform moisture content, may also be a factor in the recovery process. This recovery in fine-grained subgrade materials subjected to repeated loading after freeze-thaw cycling, has been noted by others (Bergan and Monismith 1973, MacLeod 1971). The fact that the progressive increase in the resilient modulus was observed only on the least consolidated specimens (having the highest moisture contents) would suggest partial recovery during load cycling as a plausible explanation.

For the thawed silt, resilient Poisson's ratio μ_r ranged from 0.07 to 0.61 (Table BV, App. B), the average value being 0.36. Generally, μ_r increased with increasing deviator stress and decreasing confining pressure (Fig. 24

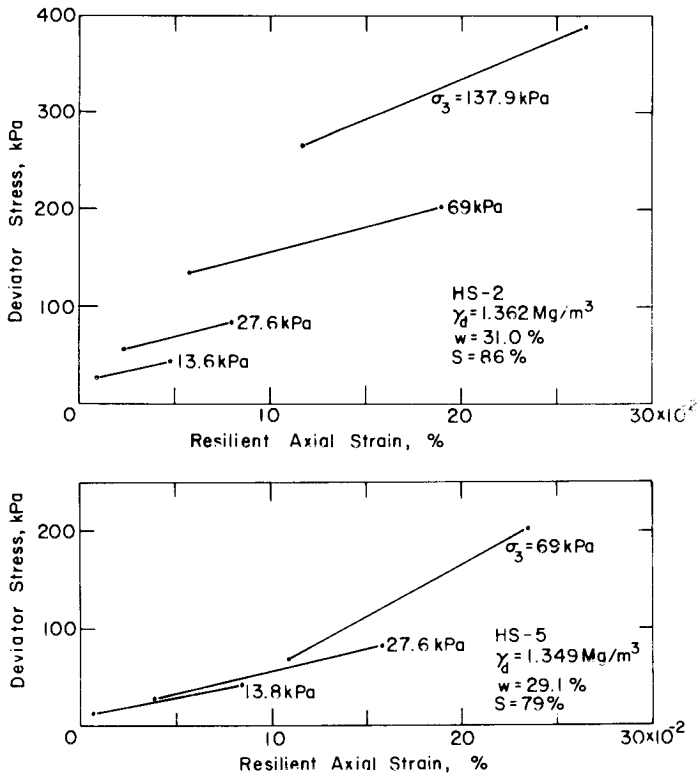

Figure 25. Resilient axial strains in two fully recovered silt specimens.

Several values of μ_r greater than 0.5 were obtained. In almost all cases the abnormally high values tended to occur at the higher deviator stress levels applied at a given confining pressure. An increase in the apparent diameter of the specimen caused by the development of vertical tension cracks in the gage length is the most probable cause of this anomaly. This conclusion also is supported by the work of MacLeod (1971), who interpreted sudden changes in μ_r as indication of specimen damage.

The results show trends similar to those reported by Nair and Chang (1973), namely an increase in μ_r and a decrease in M_r resulting from an increase in moisture content and decrease in dry density.

Four series of repeated-load triaxial tests were completed on undisturbed samples taken from the pavement subgrade in late fall when, presumably, the silt had recovered fully from the thaw-weakened state. The four specimens were tested prior to the development of the radial deformation measurement system. Specimens in the recovered state were not consolidated. Dry densities were in the same range as in the thawed, partially consolidated specimens, but the moisture contents were lower than those in thawed specimens, ranging from about 28% to 31%. The stress conditions also differed from those used in later tests on the thawed specimens. The stress conditions, test results, and specimen properties are given in Table BVI (App. B), together with calculated values of resilient modulus.

Figure 25 shows resilient axial strain for two specimens, plotted against deviator stress at various levels of confining pressure. The resilient modulus calculated for these and other specimens tends to decrease with increasing stress and to increase with increasing confining pressure. Values of the resilient modulus for these recovered silt specimens (Table BVI, App. B) were generally an order of magnitude greater than for thawed specimens, ranging from about 53 MPa to 345 MPa.

A notable exception is specimen HS-3, for which a modulus of more than 1 GPa was obtained at σ_3 = σ_d = 69 kPa. The modulus dropped to 146 MPa when the stress levels were increased to σ_3 = 137.9 kPa and σ_d = 135.8 kPa for the next segment of the test. Possibly the LVDT clamps failed to respond fully to the deformation of the specimens, but this supposition cannot be verified.

Silt – statistical analysis

Values of resilient modulus M_r and Poisson's ratio μ_r of frozen, thawed, and recovered silt, calculated from

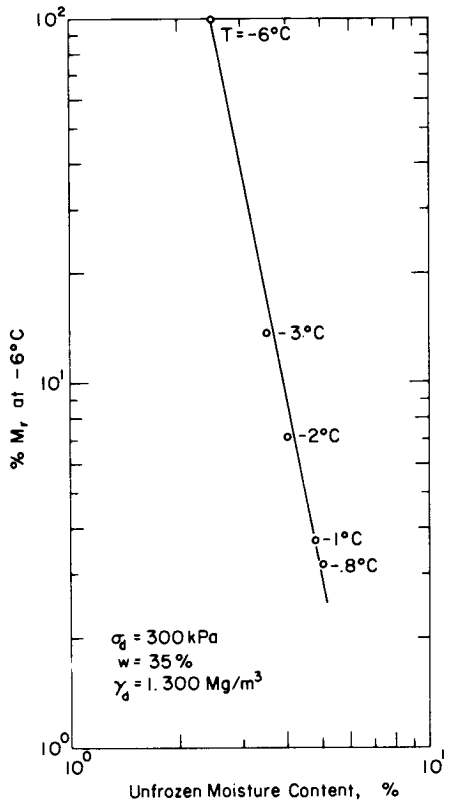

Figure 26. Variation in resilient modulus of frozen silt with unfrozen moisture content.

the test results (App. B), were correlated with the stress parameters confining stress σ_3 and deviator stress σ_d, or with the sum of the principal stresses θ and the principal stress ratio σ_1/σ_3, and with the material parameters moisture content w and dry density γ_d (App. C). For frozen silt the moduli were correlated also with temperature.

Four equations are given in Appendix C that represent attempts to model the resilient response of the frozen silt. The equation:

$$\ln M_r = 68.442 - w^2\,(8.008\times10^{-3}) - \gamma_d\,(33.267) -$$

$$- \sigma_d\,(7.106\times10^{-3}) + \sigma_d^2\,(7.652\times10^{-6}) - T(.662)$$

was chosen since it has the highest correlation coefficient (R^2 = 0.87), with a standard error of 0.513. All stresses and M_r are expressed in kPa, w in percent, γ_d in Mg/m^3, and T in °C. The most significant term in the equation is temperature. The ranges of validity of the expression are $-6.5°C \leq T \leq -0.5°C$, $35.3\% \leq w \leq 40.0\%$ and $1.214\ \text{Mg/m}^3 \leq \gamma_d \leq 1.301\ \text{Mg/m}^3$. The range of deviator stresses for which the expression is valid varies with test temperature (Table BIV). No meaningful correlation was found between M_r of the frozen silt and confining pressure σ_3. Table BIV (App. B) shows that σ_3 was varied only in the tests on one of the specimens, and little or no effect on M_r was found except at the highest temperature.

It is known that moist or saturated soils at temperatures below 0°C may contain varying amounts of unfrozen water (Tice et al. 1976). As the test results reported herein and the regression equation show a strong dependence of the resilient modulus M_r of the frozen silt on temperature, it was considered to be of interest to seek a relationship between M_r and the unfrozen moisture content. Tice et al. (1976) made laboratory determinations of the unfrozen water content of a number of soils at various temperatures below freezing, and used linear regression techniques to analyze the phase composition data of each soil, resulting in phase composition curves showing unfrozen water content vs temperature. Values of unfrozen water content corresponding to several temperatures were obtained from the phase composition curve of a silt similar to the one tested here. The resilient modulus M_r of the silt was then calculated for each of those temperatures from the regression equation of M_r for the frozen silt.

Figure 26 shows the plot (log-log scale) of the resilient modulus in percent of the resilient modulus at -6°C vs the unfrozen moisture content in percent. The significant influence of small changes in the unfrozen moisture content on the resilient modulus of the silt is evident. An increase from 2.5 to 5.0% in unfrozen moisture content (corresponding to a temperature change of -6.0° to -0.8°C) is reflected in a drop of about 97% in M_r.

The resilient axial response of the thawed silt was best characterized by expressions containing ln M_r as the dependent variable. Two equations for ln M_r (App. C) resulted in almost identical values of the correlation coefficients and standard errors.

The selected equation for thawed silt is:

$$\ln M_r = -58.906 + w(2.997) - w^2\,(4.208\times10^{-2}) +$$

$$+ \gamma_d\,(12.355) - \sigma_1/\sigma_3\,(1.232) + (\sigma_1/\sigma_3)^2\,(.201) +$$

$$+ \theta\,(2.377\times10^{-3})$$

where θ is the sum of the principal stresses, M_r and all stresses are expressed in kPa, moisture content in percent, and dry density in Mg/m^3. The correlation coefficient is relatively low (R^2 = 0.47), indicating scatter in the test results. The variations inherent in

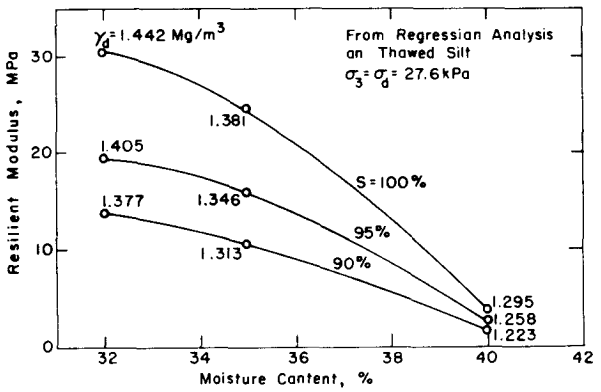

Figure 27. Influence of moisture content and dry density on the resilient modulus of thawed silt.

undisturbed specimens of this type are undoubtedly a factor here. However, the relative effect of the main variables on the resilient modulus is apparent in the expression. Moisture content is the most significant single factor affecting M_r. Figure 27 shows the effect of w upon the resilient modulus given by the regression equation, using compatible values of dry density corresponding to 90, 95, and 100% saturation, and holding the confining pressure and deviator stress constant at 27.6 kPa.

The resilient Poisson's ratio of the thawed silt is best characterized by the following equation:

$$\ln \mu_r = 51.502 - w(2.67) + w^2(3.69\times10^{-2}) -$$

$$- \gamma_d^2(2.528) - \sigma_3^2(5.119\times10^{-5}) + \sigma_d(6.084\times10^{-3})$$

where, as before, stresses are expressed in kPa, w in percent, and γ_d in Mg/m^3. The correlation coefficient (R^2 = 0.23) and standard error (0.49) indicate a great deal of scatter in the test data. The general tendency of μ_r to increase with increasing deviator stress and decreasing confining stress is apparent in the signs of the coefficients. The influence of w and γ_d on μ_r is ambiguous; as w increases within the limits of 31% to 39% and γ_d decreases (assuming the degree of saturation remains unchanged), the net effect on μ_r will be first a decrease and then an increase.

The resilient behavior of the silt in the recovered state is best characterized as

$$M_r = -7.198\times10^5 + \gamma_d^2(5.05\times10^5) + \sigma_3(1.483\times10^4)$$

$$- \sigma_3^2(76.17) - \sigma_d(6.234\times10^3) + \sigma_d^2(11.89)$$

where M_r and all stresses are expressed in kPa, and the dry density is expressed in Mg/m^3. Unfortunately the

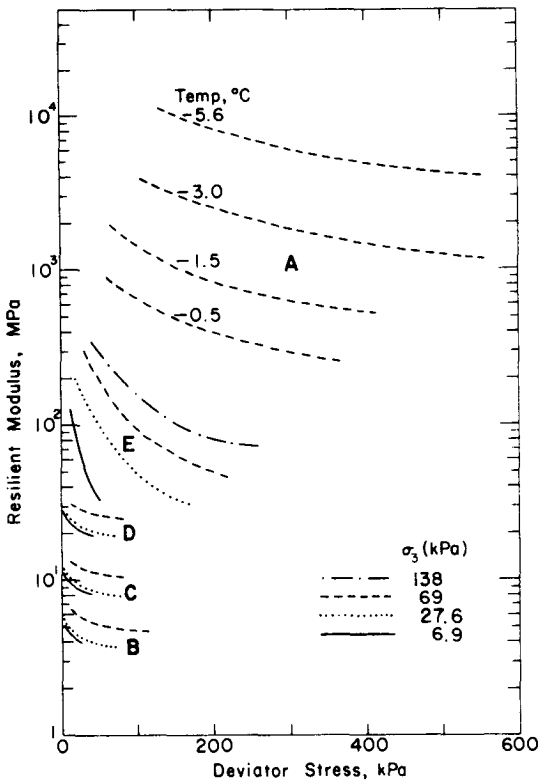

Curve	Description	w (%)	S (%)	γ_d (Mg/m^3)
A	Frozen	40	95	1.218
B	Thawed, unconsolidated	39	95	1.290
C	Thawed, partially consolidated	35	90	1.314
D	Thawed, partially consolidated	32	97	1.426
E	Fully recovered	29	80	1.346

Figure 28. Resilient modulus of silt from repeated-load triaxial tests.

specimens that were tested ranged in moisture content only from about 28 to 31%, an insufficient range for ascertaining the dependence of M_r on moisture content. Hence, this expression is of limited usefulness. Considerable scatter in the test data is evidenced by the values of the correlation coefficients (R^2 = 0.48) for the regression equation.

The regression equations developed for frozen, thawed, and recovered silt were employed to generate an illustrative diagram with resilient modulus plotted against deviator stress (Fig. 28). Values of the material parameters were selected primarily on the basis of the reductions in the moisture content (40% to 29%) observed in the test specimens representing the progressive

transformation of the soil from the frozen to the recovered state. Compatible dry densities were then selected for calculation of resilient moduli by means of the regression equations.

It can be seen that there is a considerable range of M_r over the frozen, thawed and recovered states. M_r can change from more than 1×10^4 MPa for the frozen condition, to less than 4 MPa for the thawed condition, and then to more than 3×10^2 MPa for the fully recovered condition.

DISCUSSION AND CONCLUSIONS

From Figure 12 and Figure A7 (App. A) it can be seen that resilient moduli of the silt obtained from the analysis of the field test results vary from a minimum of approximately 1-2 MPa in the thin thawed layer at the beginning of subgrade thawing, to 80-200 MPa in the fully recovered condition. Analysis of laboratory test results (Fig. 28) showed M_r for the unconsolidated condition immediately after thawing to be about 4 MPa, while the value for the fully recovered state ranged from 30 to 300 MPa depending on the deviator and confining stress levels. It thus appears that the repeated-load triaxial testing techniques employed in this research can adequately obtain M_r values for the range of seasonal conditions, providing that conditions of moisture are known or can be accurately estimated.

More direct comparison of the moduli determined by the two procedures, for further validation of the laboratory repeated-load triaxial test method, would require a suitable nondestructive and accurate measure of changes in moisture content during the series of field tests. Alternatively, it may be possible to bridge from the moisture content-dependent laboratory values of M_r to the time-dependent field values by means of laboratory consolidation tests in which time of consolidation and moisture content would be related. This question is of interest because it raises the possibility of determining a complete set of resilient modulus vs time-of-recovery data for pavement design from laboratory repeated-load triaxial tests of the type described herein and conventional consolidation tests. This proposition will be examined in a continuing phase of the investigations.

The research results summarized herein lead to the following conclusions:

1. A reasonable measure of the resilient modulus of silt subgrade soil can be obtained from deflections measured in plate-bearing tests on the surface of an all-bituminous-concrete pavement. The rate of recovery from the thaw-weakened condition can be determined by performing such tests throughout the thawing and recovery periods. The resilient modulus of the silt underlying the test pavements in Hanover, New Hampshire, ranges from about 1-2 MPa during thawing, 80-200 MPa in the fully recovered state, and to more than 10,000 MPa when frozen.

2. Recovery of the resilient modulus after thawing occurs at a low rate and continues throughout the summer and fall. While the minimum resilient modulus of the silt immediately after thawing decreased to as little as 1 to 2% of the fully recovered value, the modulus had reached only 5 to 10% of the recovered value by about 20 days after thawing and only 12 to 20% about 60 days after thawing.

3. Resilient moduli of the silt subgrade soil calculated from plate-bearing tests on the 127-mm pavement show a more even progression of recovery with time, compared with tests on the 229-mm pavement. Also, the observed deflection basin for the 127-mm pavement are more closely matched by the deflection basins calculated on the basis of test values of resilient modulus of asphalt concrete, compared with the observed and calculated deflection basins for the 229-mm pavement. Accordingly, it appears advantageous to conduct tests of this type on relatively thin asphalt concrete pavements.

4. The resilient modulus and Poisson's ratio of silt in the various stages of the freeze-thaw cycle can be determined by repeated-load triaxial tests on samples obtained undisturbed while frozen, and tested in the frozen condition, after thawing when strength is sufficient, and during the recovery phases. Specimens of silt from the test pavements in Hanover were too soft immediately after thawing to be tested, and first had to be partially consolidated; thus it was not possible to determine the minimum resilient modulus matching the minimum values obtained in the plate-bearing tests shortly after thawing of the silt began.

5. Values of resilient modulus determined by repeated-load triaxial tests on frozen silt from the test pavements ranged from about 1 to 40 GPa, at temperatures of -0.7 to $-6.5°C$. The regression equations developed from tests in the thawed and recovered conditions show that at prevailing moisture contents and compatible dry densities the resilient modulus ranges from less than 4 MPa after thawing to about 30 to 300 MPa when fully recovered, depending on stress levels.

6. The resilient modulus and Poisson's ratio of silt determined in repeated-load triaxial tests can be expressed as a function of deviator stress, minor principal stress, moisture content, and dry density. In the frozen condition an additional parameter, temperature, is the most significant variable.

7. Under given stress conditions, the resilient modulus of silt during recovery after thaw can be modelled as a function of changes in moisture content that take place during consolidation.

LITERATURE CITED

Allen, J.J. and M.R. Thompson (1974) The resilient response of granular materials subjected to time-dependent lateral stresses. Presented at the 53rd Annual Meeting, Highway Research Board, Washington, D.C.

American Association of State Highway and Transportation Officials -- AASHTO (1974) Standard specifications for transportation materials and methods of sampling and testing. AASHTO, Washington, D.C.

Barenberg, E.J. (1973) Mathematical modeling of pavement systems: State-of-the-art. *Proceedings of the Allerton Park Conference on Systems Approach to Airfield Pavements.* U.S. Army Construction Engineering Research Laboratory, Technical Report P-5.

Barker, W.R. and W.N. Brabston (1974) Development of a structural design procedure for flexible airport pavement. U.S. Army Engineer Waterways Experiment Station (USAE WES) report prepared for Federal Aviation Agency, Report No. FFA-RD-74.

Bergan, A.T. (1972) Some considerations in the design of asphalt concrete pavements for cold regions. Ph. D. Dissertation, University of California, Berkeley.

Bergan, A.T. and C.L. Monismith (1972) Some fatigue considerations in the design of asphalt concrete pavements. *Proceedings, Canadian Technical Asphalt Association,* vol. XVII.

Bergan, A.T. and C.L. Monismith (1973) Characterization of subgrade soils in cold regions for pavement design purposes. Highway Research Record 431.

Culley, R.W. (1970) Effect of freeze-thaw cycling on stress-strain characteristics and volume change of a till subjected to repetitive loading. Saskatchewan Department of Highways, Technical Report 13.

Eaton, R. and D. VanPernis (1973) USA CRREL highway pavement test sections. Organization for Economic Cooperation and Development (OECD) Symposium on Frost Action on Roads, Oslo, Norway.

Gibra, Isaac N. (1973) *Probability and statistical inference for scientists and engineers.* New Jersey: Prentice-Hall, Inc.

Hicks, R.G. (1970) Factors influencing the resilient properties of granular materials. Ph. D. Dissertation, University of California, Berkeley.

Johnson, T.C., R.L. Berg, K.L. Carey and C.W. Kaplar (1975) Roadway design in seasonal frost areas. CRREL Technical Report 259, and TRB Synthesis of Highway Practice No. 26. AD A010633.

Kasianchuk, D.A. (1968) Fatigue considerations in the design of asphalt concrete pavements. Ph. D. Dissertation, University of California, Berkeley.

MacLeod, D.R. (1971) Some fatigue considerations in the design of thin pavements. M. Sc. Thesis, University of Saskatchewan, Saskatoon.

McLeod, N.W. (1972) A 4-year survey of low-temperature transverse pavement cracking on three Ontario test roads. *Proceedings, Association of Asphalt Paving Technologists,* vol. 41.

Michelow, J. (1963) Analysis of stresses and displacements in an *n*-layered elastic system under a load uniformly distributed on a circular area. California Research Corporation, Richmond, California.

Mickleborough, B.W. (1970) An experimental study of the effects of freezing on clay subgrades. M.Sc. Thesis, University of Saskatchewan, Saskatoon.

Monismith, C.L. and K.E. Secor (1972) Viscoelastic behavior of asphalt concrete pavements. *Proceedings, First International Conference on Structural Design of Asphalt Pavements,* University of Michigan.

Nair, K. and C.Y. Chang (1973) Flexible pavement design and management, materials characterization. National Cooperative Highway Research Program Report 140.

Pagen, C.A. and V.K. Khosla (1968) Frost action characteristics of compacted cohesive soil. Ohio State University Report no. EES 248-4.

Pell, P.S. and S.F. Brown (1972a) A fundamental structural design procedure for flexible pavements. Third International Conference on the Structural Design of Asphalt Pavements, University of Michigan, p. 369-381.

Pell, P.S. and S.F. Brown (1972b) The characterization of materials for the design of flexible pavement structures. Third International Conference on the Structural Design of Asphalt Pavements, University of Michigan, p. 326-342.

Quinn, W.F., D. Carbee and T.C. Johnson (1973) Membrane-encapsulated soil layers (MESL) for road construction in cold regions. Organization for Economic Cooperation and Development Symposium on Frost Action on Roads, Oslo, Norway.

Robnett, Q.L. and M.R. Thompson (1976) Effect of lime treatment on the resilient behavior of fine-grained soils. Transportation Research Board Record 560.

Sayegh, B. (1967) Viscoelastic properties of bituminous mixes. *Proceedings, Second International Conference on Structural Design of Asphalt Pavements,* University of Michigan.

Schmidt, R.J. and P.E. Graf (1972) The effect of water on the resilient modulus of asphalt-treated mixes. *Proceedings, Association of Asphalt Paving Technologists,* vol. 41.

Schmidt, R.J. (1974) The effect of temperature, freeze-thaw, and various moisture conditions on the resilient modulus of asphalt-treated mixes. Transportation Research Record no. 515.

Seed, H.B., C.K. Chan and C.L. Monismith (1955) Effects of repeated loading on the strength and deformation of compacted clay. *Proceedings, Highway Research Board,* vol. 34, p. 541-558.

Shackel, B. (1973) Repeated loading of soils -- A review. Australian Road Research, vol. 5, no. 3.

Smith, N. and J.A. Groves (1976) Analysis of flexible pavement resilient surface deformation using the chevron layered elastic analysis computer program. Symposium on Non-destructive Test and Evaluation of Airport Pavement, 18-20 November 1975, USAE WES.

Stevens, H.W. (1975) The response of frozen soils to vibratory loads. CRREL Technical Report 265. (AD A013831).

Tice, A.R., D.M. Anderson and A. Banin (1976) The prediction of unfrozen water contents in frozen soils from liquid limit determinations. CRREL Report 76-8. (AD A026632).

Warren, H.W. and W.L. Dieckmann (1963) Numerical computation of stresses and strains in a multiple-layered asphalt pavement system. California Research Corporation, Richmond, California.

APPENDIX A. REPEATED-LOAD PLATE-BEARING TEST RESULTS

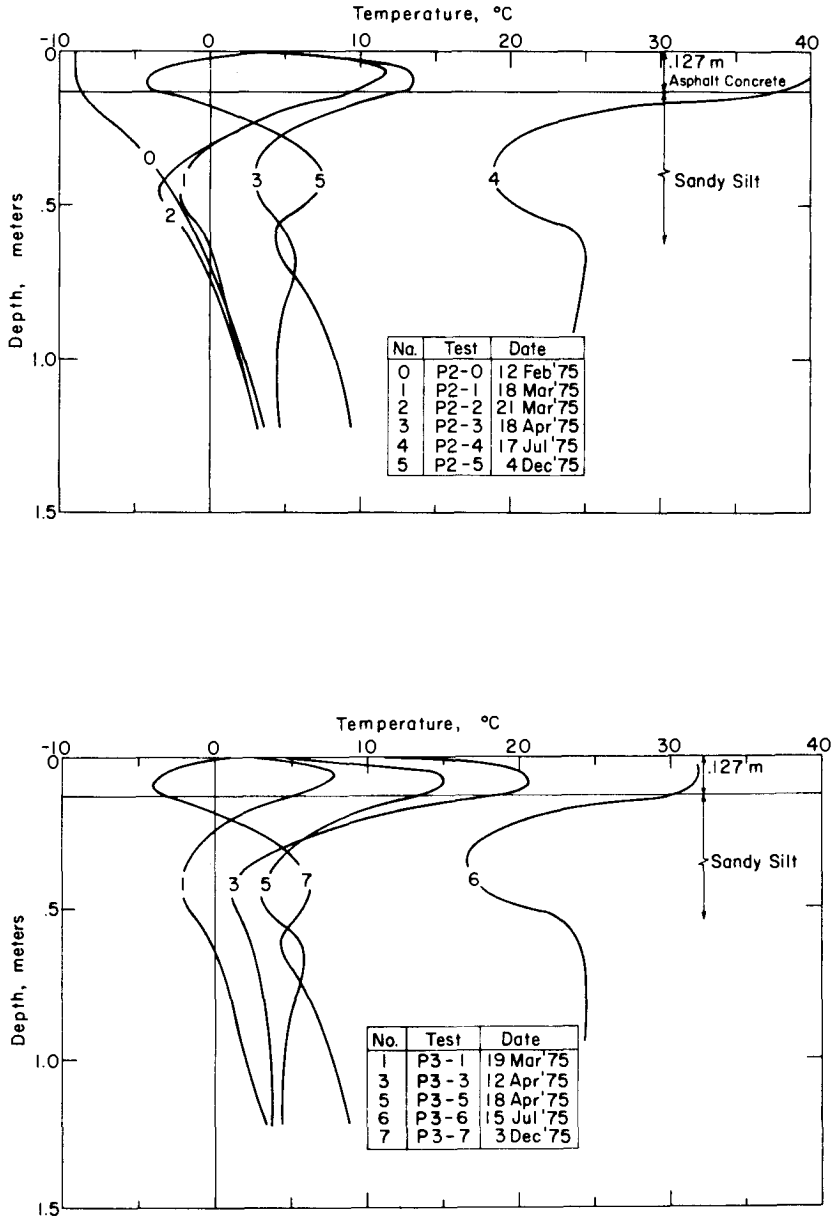

Figure A1. Ground temperatures at test points P2 and P3.

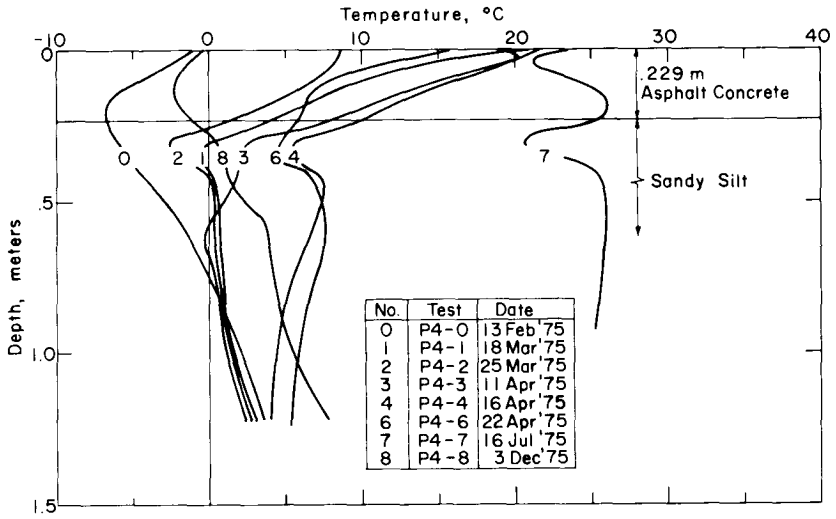

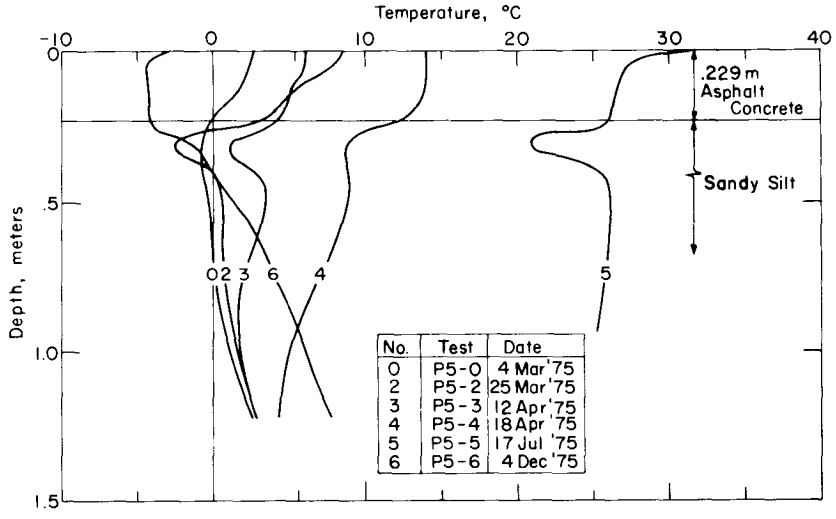

Figure A2. Ground temperatures at test points P4 and P5.

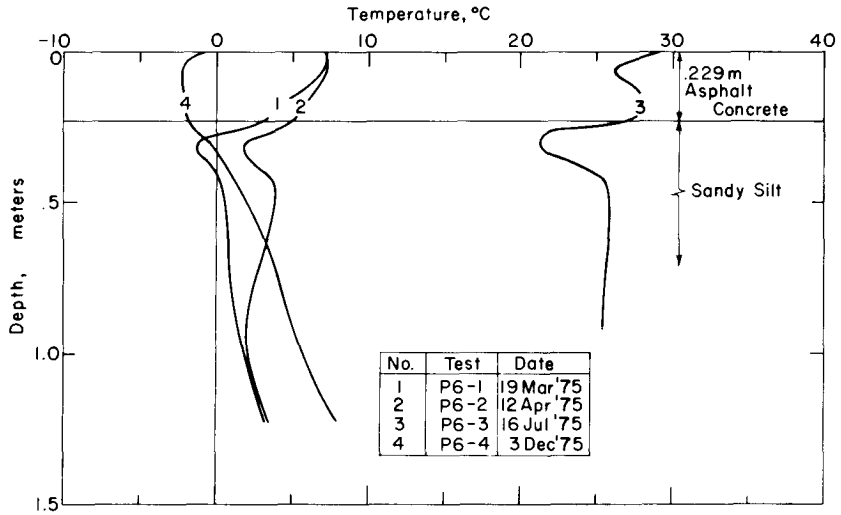

Figure A3. Ground temperatures at test point P6.

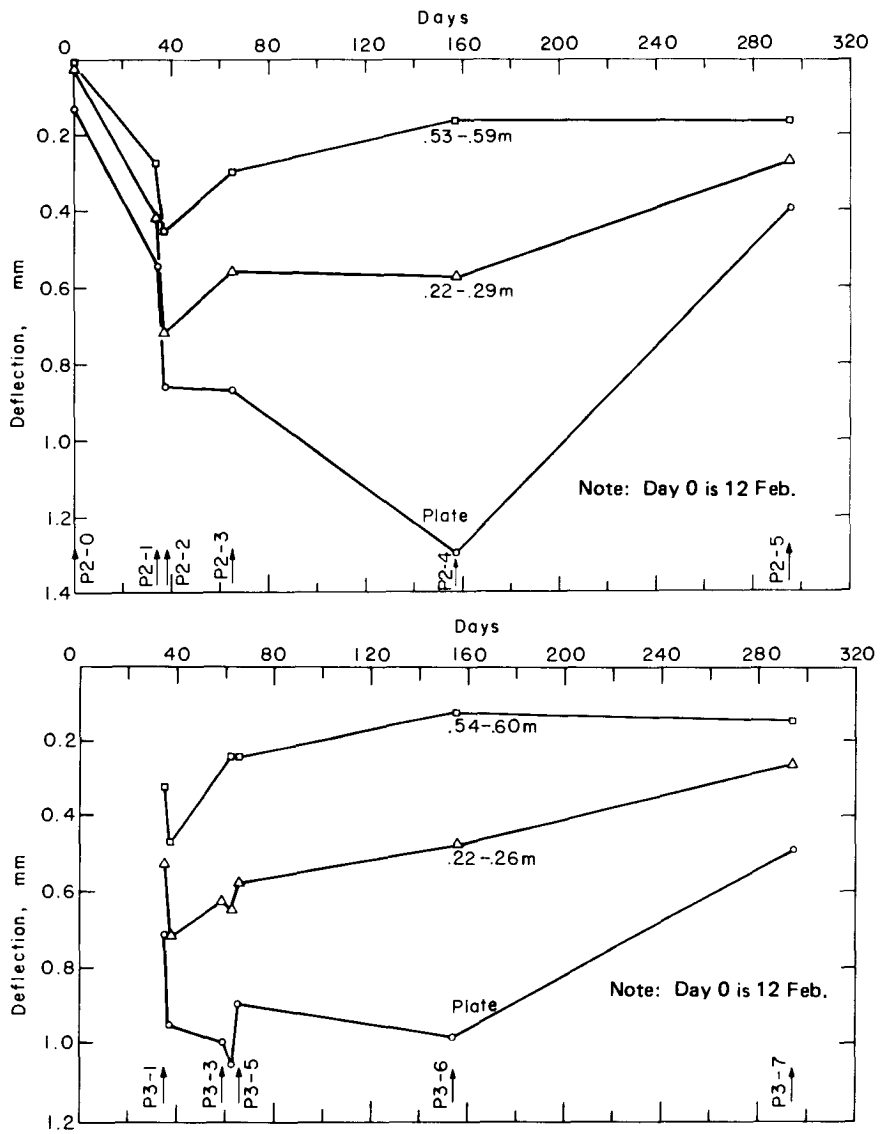

Figure A4. Resilient deflection of plate and two radial points, test points P2 and P3.

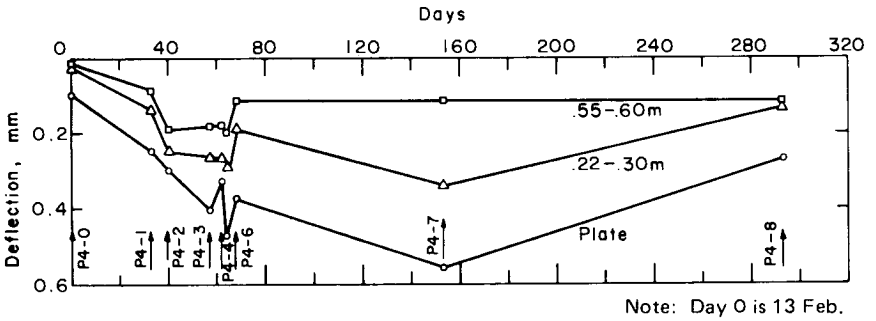

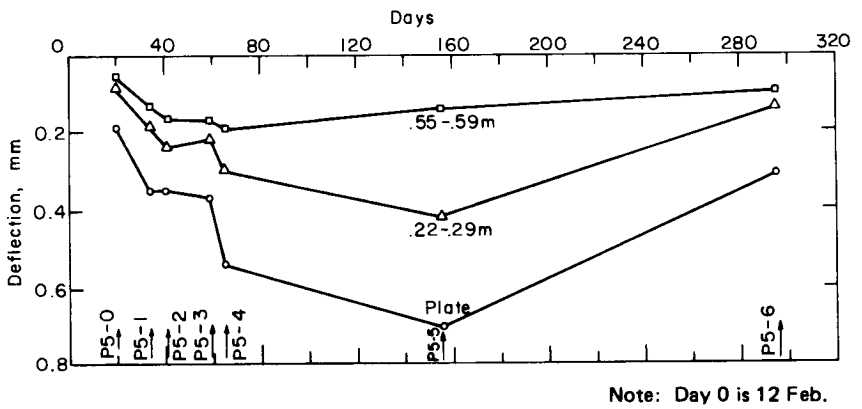

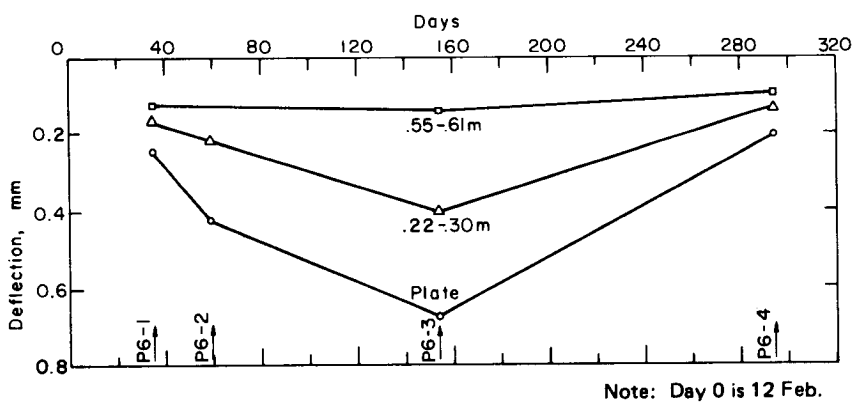

Figure A5. Resilient deflection of plate and two radial points, test points P4, P5 and P6.

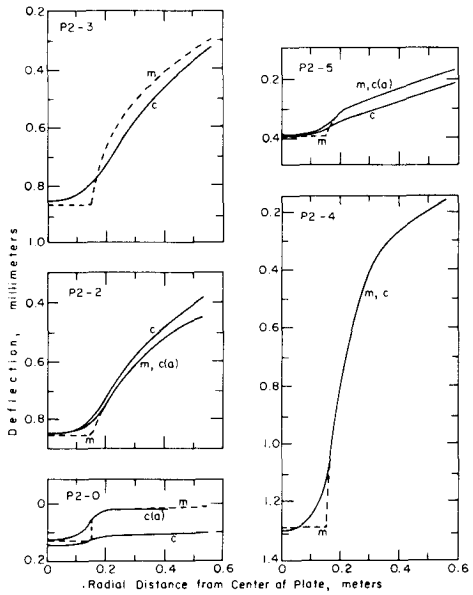

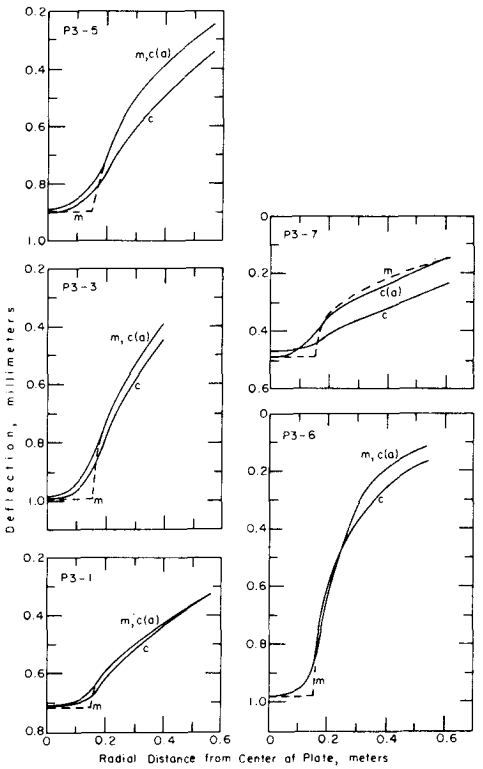

m — measured
c — calculated
c(a) — calculated (adjusted)

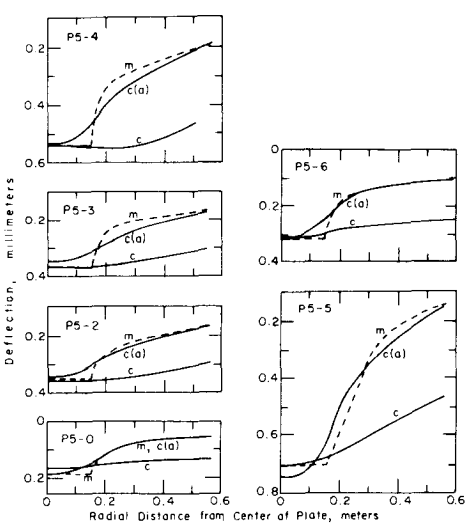

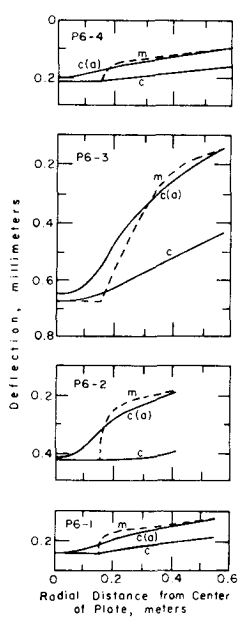

Figure A6. Measured and calculated deflection basins, test points P2, P3, P5 and P6.

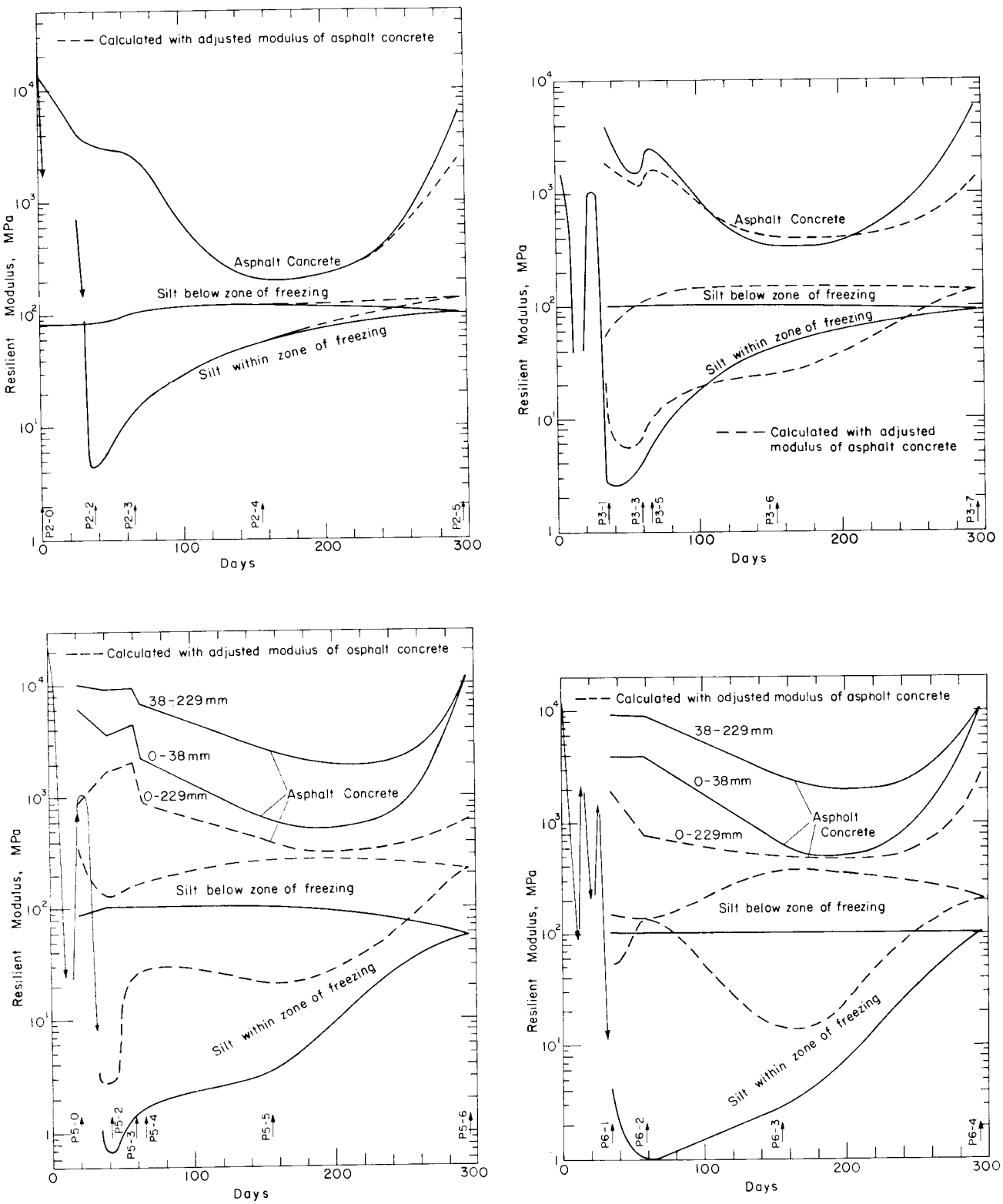

Figure A7. Calculated resilient moduli of subgrade silt, and moduli of asphalt concrete used in analyses, test points P2, P3, P5 and P6.

APPENDIX B. LABORATORY REPEATED-LOAD TRIAXIAL TEST RESULTS

Table B1. Results of laboratory repeated-load triaxial tests on unfrozen asphalt concrete.

Sample	Confining pressure (kPa)	Deviator stress (kPa)	Radial strain (%)	Axial strain (%)	Resilient Poisson's ratio	Resilient modulus (GPa)	Density (Mg/m^3)	Moisture content (%)	Test temperature (°C)
FD-9-2A	103.4	104.8	0.002	0.006	0.33	1.747	2.389	0.40	15.8
		104.8	0.010	0.027	0.37	0.388		0.40	32.2
		106.2	0.014	0.069	0.20	0.154		1.26	33.1
		202.7	0.004	0.016	0.25	1.267		1.26	15.6
		241.3	0.010	0.047	0.21	0.513		1.26	25.0
		225.5	0.009	0.033	0.27	0.683		0.32	25.6
		113.1	0.009	0.033	0.27	0.343		0.32	35.0
		206.9	0.003	0.008	0.38	2.586		0.32	15.0
FD-9-4A	103.4	213.7	0.007	0.023	0.30	0.929	2.428	0.38	23.9
		106.9	0.008	0.047	0.17	0.227		0.38	32.8
		217.9	0.005	0.014	0.36	1.556		0.38	15.6
		216.5	0.016	0.052	0.31	0.416		0.90	22.2
		105.5	0.019	0.064	0.30	0.165		0.90	30.6
		220.6	0.004	0.027	0.15	0.817		0.90	15.6
		208.9	0.010	0.026	0.38	0.803		0.51	23.9
		122.7	0.015	0.058	0.26	0.212		0.51	33.3
		217.2	0.002	0.018	0.11	1.207		0.51	15.6
FD-9-1B	103.4	104.8	0.019	0.041	0.46	0.256	2.428	0.40	33.1
		209.6	0.004	0.014	0.29	1.497		0.40	15.6
		213.7	0.009	0.019	0.47	1.124		0.40	22.2
		213.0	0.017	0.040	0.43	0.533		0.94	25.0
		212.4	0.008	0.020	0.40	1.062		0.94	17.8
		106.2	0.022	0.048	0.46	0.221		0.94	33.3
		224.8	0.020	0.044	0.45	0.511		0.54	25.6
		109.6	0.022	0.046	0.48	0.238		0.54	33.3
		218.6	0.005	0.017	0.29	1.286		0.54	16.7
FD-9-3B	103.4	206.2	0.002	0.010	0.20	2.062	2.442	0.40	15.8
		97.2	0.013	0.029	0.45	0.335		0.40	33.9
		215.8	0.007	0.024	0.29	0.899		1.01	22.2
		109.6	0.019	0.038	0.50	0.288		1.01	32.2
		117.9	0.005	0.012	0.42	0.983		1.01	15.6
		208.9	0.009	0.019	0.47	1.099		0.65	24.4
		113.8	0.019	0.051	0.37	0.223		0.65	33.1
		217.2	0.005	0.018	0.28	1.207		0.65	15.6
FD-5-1	103.4	211.7	0.007	0.015	0.47	1.411	2.402	0	23.9
		105.5	0.008	0.027	0.30	0.391		0	32.2
		215.8		0.010		2.158		0	15.6
		213.7	0.012	0.043	0.28	0.497		1.44	23.9
		104.1	0.012	0.045	0.27	0.231		1.44	32.8
		217.2	0.005	0.016	0.31	1.358		1.44	15.6
		226.8	0.008	0.022	0.36	1.031		0.71	24.4
		103.4	0.010	0.039	0.26	0.265		0.71	32.8
		219.3	0.002	0.012	0.17	1.828		0.71	15.6
FD-5-2	103.4	196.5	0.003	0.010	0.30	1.965	2.402	0.32	15.8
		97.9	0.013	0.028	0.46	0.350		0.32	32.2
		211.7	0.022	0.042	0.52	0.504		1.40	23.3
		215.8	0.009	0.020	0.45	1.079		1.40	15.6
		117.2	0.025	0.043	0.58	0.273		1.40	32.2
		215.1	0.002	0.003	0.67	7.170		1.40	5.0
		217.9	0.014	0.026	0.54	0.838		0.90	22.8
		108.2	0.020	0.041	0.49	0.264	2.381	0.90	33.1
		217.2	0.006	0.013	0.46	1.671		0.90	15.6

Table BI (cont'd). Results of laboratory repeated-load triaxial tests on unfrozen asphalt concrete.

Sample	Confining pressure (kPa)	Deviator stress (kPa)	Radial strain (%)	Axial strain (%)	Resilient Poisson's ratio	Resilient modulus (GPa)	Density (Mg/m^3)	Moisture content (%)	Test temperature (°C)
FD-5-3	103.4	193.1	0.004	0.009	0.44	2.146		0.24	15.6
		100.7	0.016	0.025	0.64	0.403		0.24	33.6
		213.0	0.003	0.012	0.25	1.775		1.07	15.6
		102.7	0.015	0.035	0.43	0.293		1.07	33.9
		214.4	0.008	0.019	0.42	1.128		1.07	22.2
		218.6	0.011	0.018	0.61	1.214		0.57	21.1
		111.0	0.015	0.030	0.50	0.370		0.57	33.3
		212.4	0.005	0.012	0.42	1.770		0.57	15.6
FD-9-2B	103.4	222.7	0.013	0.047	0.28	0.474	2.458	0.24	25.6
		115.8	0.016	0.045	0.36	0.257		0.24	32.2
		231.7	0.003	0.015	0.20	1.545		0.24	15.6
		216.5	0.022	0.057	0.39	0.380		2.04	23.9
		100.5	0.026	0.061	0.43	0.165		2.04	33.3
		212.4	0.008	0.025	0.32	0.850		2.04	15.6
		218.6	0.014	0.035	0.40	0.625		1.09	25.8
		107.6	0.015	0.030	0.50	0.359		1.09	33.1
		217.9	0.004	0.009	0.44	2.421		1.09	15.6
		217.9		0.003		7.263		1.09	5.0

Table BII. Results of laboratory repeated-load triaxial tests on frozen asphalt concrete.

Sample	Confining pressure (kPa)	Deviator stress (kPa)	Axial strain (%)	Resilient modulus (GPa)	Density (Mg/m^3)	Moisture content (%)	Test temperature (°C)
FD-9-2A	103.4	318.5	0.0018	17.690	2.393	1.26	-6.7
		216.5	0.0022	9.841		0.32	-5.6
FD-9-4A	103.4	222.7	0.0025	8.908	2.428	0.38	-6.7
		218.6	0.0022	9.936		0.90	-6.7
		215.1	0.0015	14.340		0.51	-6.7
FD-9-1B	103.4	201.3	0.0020	10.070	2.428	0.40	-6.7
		211.7	0.0019	11.140		0.94	-3.9
		218.6	0.0027	8.096		0.54	-6.7
FD-9-2B	103.4	222.0	0.0015	14.800	2.458	0.24	-6.7
		212.4	0.0015	14.160		2.04	-6.7
		222.7	0.0015	14.850		1.09	-5.6
FD-9-3B	103.4	193.8	0.0011	17.620	2.442	0.40	-6.7
		217.9	0.0019	11.470		1.01	-6.7
		226.8	0.0016	14.180		0.65	-6.7
FD-5-1	103.4	220.0	0.0022	10.000	2.402	0	-6.1
		217.2	0.0014	15.510		1.44	-6.7
		216.5	0.0020	10.830		0.71	-5.6
FD-5-2	103.4	211.7	0.0018	11.760	2.402	0.32	-6.7
		217.2	0.0028	7.757		0.90	-6.7
FD-5-3	103.4	193.1	0.0020	9.655	2.373	0.24	-6.7
		213.7	0.0021	10.180		1.07	-6.7
		221.3	0.0023	9.622		0.57	-6.7

Table BIII. Results of laboratory repeated-load triaxial tests on air-dry asphalt concrete.

Sample	Confining pressure (kPa)	Deviator stress (kPa)	Axial strain (%)	Resilient modulus (GPa)	Density (Mg/m^3)	Test temperature (°C)
FD-9-0A	310.3	110.1	0.0007	15.730	2.310	-6.7
	103.4	110.1	0.0007	15.730		
	310.3	307.5	0.0021	14.640		
	310.3	405.4	0.0027	15.010		
	103.4	307.5	0.0021	14.640		
	103.4	405.4	0.0027	15.010		
	310.3	110.1	0.0052	2.117		15.6
	103.4	110.1	0.0052	2.117		
	310.3	306.1	0.0156	1.962		
	310.3	403.4	0.0225	1.793		
	103.4	305.4	0.0173	1.765		
	103.4	402.0	0.0209	1.923		
	310.3	108.9	0.0206	0.529		32.2
	103.4	108.3	0.0207	0.523		
	310.3	298.6	0.0558	0.535		
FD-9-0B	310.3	110.1	0.0006	18.390	2.418	-6.7
	103.4	110.1	0.0006	18.390		
	103.4	306.1	0.0015	20.410		
	310.3	404.0	0.0022	18.360		
	103.4	306.1	0.0015	20.410		
	103.4	404.0	0.0022	18.360		
	310.3	110.1	0.0019	5.795		15.6
	103.4	109.6	0.0019	5.768		
	310.3	305.4	0.0037	8.254		
	310.3	402.7	0.0067	6.010		
	103.4	304.8	0.0037	8.238		
	103.4	401.3	0.0075	5.351		
	310.3	108.9	0.0147	0.741		32.2
	103.4	108.3	0.0148	0.732		
	310.3	299.2	0.0372	0.804		
	310.3	392.3	0.0412	0.952		
	103.4	295.8	0.0264	1.121		
	103.4	387.5	0.0303	1.279		
FD-5-0C	310.3	111.0	0.0007	15.860	2.426	-6.7
	103.4	111.0	0.0007	15.860		
	310.3	308.2	0.0021	14.680		
	310.3	406.8	0.0028	14.530		
	103.4	328.9	0.0021	15.660		
	103.4	406.8	0.0028	14.530		
	310.3	110.3	0.0035	3.151		15.6
	103.4	110.3	0.0035	3.151		
	310.3	306.8	0.0160	1.918		
	310.3	404.0	0.0213	1.897		
	103.4	306.1	0.0178	1.724		
	103.4	404.0	0.0231	1.749		
	310.3	109.6	0.0281	0.390		32.2
	103.4	108.9	0.0353	0.309		
	310.3	299.2	0.1001	0.299		
	310.3	385.4	0.1172	0.329		
	103.4	286.8	0.1045	0.274		

Table BIV. Results of repeated-load triaxial tests on frozen silt.

Condition	Sample	Confining pressure (kPa)	Deviator stress (kPa)	Radial strain (%)	Axial strain (%)	Resilient Poisson's ratio	Resilient modulus (MPa)	Dry density (Mg/m^3)	Moisture content (%)	Saturation (%)	Test temperature (°C)
Frozen	HS-1-1	69.0	200.6		0.0023		8.722×10^3	1.239	40.03	98	-4.7
			342.0		0.0040		8.550				-4.4
			384.7		0.0045		8.549				-4.4
			657.8		0.0113		5.821				-4.4
			136.5		0.0068		2.007				-1.5
			208.2		0.0131		1.589				-1.5
			350.3		0.0278		1.260				-1.5
			426.8		0.0386		1.106				-1.5
			643.3		0.0647		0.994				-1.4
			74.5		0.0046		1.620				-0.7
			125.5		0.0134		0.937				-0.7
			202.0		0.0248		0.815				-0.8
			342.7		0.0447		0.767				-0.8
			421.3		0.0526		0.801				-0.8
			551.6		0.0721		0.765				-0.8
	HS-4-1	69.0	336.5		0.0023		14.630	1.214	39.33	91	-2.5
			423.4		0.0046		9.204				-2.5
			542.6		0.0104		5.217				-2.5
			201.2		0.0028		7.186				-1.8
			340.6		0.0069		4.936				-1.8
			404.0		0.0122		3.311				-1.6
			138.6		0.0012		11.550				-1.0
			202.0		0.0151		1.338				-1.0
			340.6		0.0278		1.225				-1.0
	HS-11-4	69.0	213.7		0.0005		42.740	1.301	35.30	88	-6.5
			358.5		0.0013		27.577				-6.5
		137.9	317.2		0.0010		31.720				-6.5
		69.0	206.9		0.0013		15.915				-3.9
			337.9		0.0025		13.516				-3.9
		103.4	103.4		0.0005		20.680				-3.9
			310.3		0.0023		13.491				-3.9
		69.0	203.4		0.0040		5.085				-2.1
			317.2		0.0142		2.234				-2.1
		103.4	103.4		0.0010		10.340				-2.1
			275.8		0.0100		2.758				-2.1
		69.0	69.0		0.0011		6.273				-0.5
			193.1		0.0158		1.222				-0.5
			317.2		0.0353		0.899				-0.5
		103.4	103.4		0.0018		5.744				-0.5
			303.4		0.0272		1.115×10^3				-0.5

Table BV. Results of repeated-load triaxial tests on thawed silt.

Condition	Sample	Confining pressure (kPa)	Deviator stress (kPa)	Radial strain (%)	Axial strain (%)	Resilient Poisson's ratio	Resilient modulus (MPa)	Dry density (Mg/m^3)	Moisture content (%)	Saturation (%)	Test temperatur (°C)
Thawed	HS-1-1	6.9	3.4	0.044	0.082	0.54	4.1	1.309	39.97	100	
			6.2	0.095	0.182	0.52	3.4				
			10.3	0.117	0.231	0.51	4.5				
			13.1	0.146	0.288	0.51	4.5				
			20.7	0.210	0.440	0.48	4.7				
		27.6	13.8	0.149	0.308	0.48	4.5				

Table BV (cont'd).

Condition	Sample	Confining pressure (kPa)	Deviator stress (kPa)	Radial strain (%)	Axial strain (%)	Resilient Poisson's ratio	Resilient modulus (MPa)	Dry density (Mg/m^3)	Moisture content (%)	Saturation (%)	Test temperature (°C)
Thawed			26.9	0.252	0.534	0.47	5.0				
			40.0	0.335	0.703	0.48	5.7				
			53.1	0.401	0.839	0.48	6.3				
			76.5	0.485	1.072	0.45	7.1				
		69.0	32.4	0.255	0.551	0.46	5.9				
			63.4	0.388	0.830	0.47	7.6				
			94.5	0.503	1.012	0.50	9.3				
			123.4	0.561	1.225	0.46	10.1				
	HS-1-2	6.9	3.4	0.011	0.032	0.34	10.6	1.333	36.73	98	
			6.9	0.039	0.092	0.42	7.5				
			9.7	0.063	0.145	0.43	6.7				
			12.4	0.080	0.179	0.45	6.9				
			20.0	0.123	0.290	0.42	6.9				
		27.6	13.1	0.043	0.125	0.34	10.5				
			25.5	0.137	0.309	0.44	8.2				
			38.6	0.221	0.440	0.50	8.8				
			49.6	0.264	0.491	0.54	10.1				
			71.7	0.341	0.581	0.59	12.3				
		69.0	33.8	0.048	0.126	0.38	26.8				
			57.9	0.127	0.249	0.51	23.2				
			88.9	0.277	0.483	0.57	18.4				
			108.9	0.398	0.776	0.51	14.0				
		103.4	43.4	0.066	0.161	0.41	27.0				
			84.8	0.181	0.393	0.46	21.6				
			113.1	0.257	0.686	0.38	16.5				
	HS-1-3	6.9	2.8	0.006	0.013	0.46	21.5	1.378	36.24	100	
			6.9	0.039	0.080	0.49	8.6				
			9.7	0.056	0.128	0.44	7.6				
			12.4	0.061	0.161	0.38	7.7				
			18.6	0.091	0.228	0.40	8.2				
		27.6	11.0	0.014	0.043	0.33	25.6				
			24.1	0.099	0.203	0.49	11.9				
			34.5	0.136	0.300	0.45	11.5				
	HS-2-2	6.9	6.9		0.005		138.0	1.440	31.18	97	
			10.3		0.010		103.0				
			13.8		0.016		82.3				
			20.0	0.002	0.026	0.08	76.9				
		27.6	12.4	0.003	0.011	0.27	112.7				
			27.6	0.009	0.038	0.24	72.6				
			38.6	0.021	0.060	0.35	64.3				
		69.0	34.5	0.008	0.018	0.44	191.7				
			69.0	0.057	0.127	0.45	54.3				
			98.6	0.152	0.318	0.48	31.0				
		103.4	53.8	0.032	0.092	0.35	58.5				
		103.4	97.9	0.121	0.255	0.48	38.4	1.440	31.18	97	
			140.7	0.177	0.337	0.53	41.8				
			173.8	0.245	0.470	0.52	37.0				
	HS-3-1	6.9	2.8	0.009	0.035	0.26	8.0	1.317	38.55	100	
			6.9	0.023	0.070	0.33	9.9				
			9.7	0.038	0.079	0.48	12.3				
			13.1	0.050	0.097	0.52	13.5				
	HS-3-2	6.9	6.9		0.007		98.6	1.341	37.84	100	
			10.3	0.006	0.036	0.17	28.6				
			13.1	0.010	0.063	0.16	20.8				
			20.0	0.026	0.132	0.20	15.2				
		27.6	13.1	0.003	0.021	0.14	62.4				
			26.2	0.010	0.067	0.15	39.1				
			40.0	0.034	0.145	0.23	27.6				

Table BV (cont'd). Results of repeated-load triaxial tests on thawed silt.

Condition	Sample	Confining pressure (kPa)	Deviator stress (kPa)	Radial strain (%)	Axial strain (%)	Resilient Poisson's ratio	Resilient modulus (MPa)	Dry density (Mg/m^3)	Moisture content (%)	Saturation (%)	Test temperature (°C)
Thawed			53.1	0.090	0.254	0.35	20.9				
		69.0	31.7	0.005	0.035	0.14	90.6				
			63.4	0.017	0.105	0.16	60.4				
			99.3	0.057	0.220	0.26	45.1				
			128.9	0.137	0.380	0.36	33.9				
		103.4	54.5	0.005	0.069	0.07	79.0				
			95.2	0.028	0.144	0.19	66.1				
			151.0	0.075	0.264	0.28	57.2				
	HS-3-3	6.9	4.1		0.009		45.6	1.371	35.15	99	
			6.9		0.019		36.3				
			10.3	0.002	0.029	0.07	35.5				
			13.1	0.004	0.040	0.10	32.8				
			19.3	0.010	0.066	0.15	29.2				
		27.6	13.8	0.003	0.025	0.12	55.2				
			25.5	0.005	0.057	0.09	44.7				
			37.9	0.013	0.091	0.14	41.6				
			54.5	0.036	0.164	0.22	33.2				
			77.2	0.145	0.336	0.43	23.0				
		69.0	33.8	0.003	0.044	0.07	76.8	1.371	35.15	99	
			66.2	0.023	0.115	0.20	57.6				
			94.5	0.065	0.223	0.29	42.4				
		103.4	55.8	0.006	0.070	0.09	79.7				
			95.2	0.027	0.151	0.18	63.0				
			137.9	0.128	0.356	0.36	38.7				
	HS-4-1	6.9	3.4	0.002	0.012	0.17	28.3	1.327	35.67	94	
			6.9	0.011	0.048	0.23	14.4				
			9.7	0.018	0.074	0.24	13.1				
			14.5	0.038	0.118	0.32	12.3				
			20.0	0.070	0.179	0.39	11.2				
		27.6	13.1	0.012	0.069	0.17	19.0				
			26.2	0.078	0.232	0.34	12.3				
			40.0	0.183	0.396	0.46	10.1				
		69.0	32.4	0.067	0.165	0.41	19.6				
			62.1	0.297	0.590	0.50	10.5				
	HS-9-1	6.9	3.4	0.011	0.018	0.61	18.9	1.370	31.51	82	
			6.9	0.024	0.057	0.42	12.1				
		6.9	10.3	0.040	0.112	0.36	9.2				
			14.5	0.056	0.151	0.37	9.6				
			22.1	0.075	0.225	0.33	9.8				
		27.6	13.1	0.036	0.095	0.38	13.8				
			24.1	0.100	0.267	0.38	9.0				
			35.9	0.127	0.294	0.43	12.2				
			49.6	0.163	0.372	0.44	15.2				
	HS-9-2	6.9	2.8	0.013	0.038	0.34	7.4	1.370	33.63	93	
			6.9	0.037	0.098	0.38	7.0				
			9.7	0.047	0.134	0.35	7.2				
		27.6	12.4	0.069	0.190	0.36	6.5				
			18.6	0.096	0.273	0.35	6.8				
			12.4	0.052	0.156	0.33	7.9				
			25.5	0.115	0.319	0.36	8.0				
			39.3	0.151	0.434	0.35	9.1				
			49.6	0.155	0.439	0.35	11.3				
			72.4	0.237	0.651	0.36	11.1				
		69.0	31.0	0.085	0.269	0.32	11.5				
			61.4	0.176	0.486	0.36	12.6				
			86.9	0.243	0.635	0.38	13.7				

Table BV (cont'd).

Condition	Sample	Confining pressure (kPa)	Deviator stress (kPa)	Radial strain (%)	Axial strain (%)	Resilient Poisson's ratio	Resilient modulus (MPa)	Dry density (Mg/m^3)	Moisture content (%)	Saturation (%)	Test temperature (°C)
Thawed	HS-9-4	6.9	3.4	0.006	0.014	0.43	24.3	1.419	32.16	97	
			7.6	0.024	0.055	0.44	13.8				
			11.0	0.049	0.099	0.50	11.1				
			13.1	0.071	0.140	0.51	9.4				
			19.3	0.112	0.220	0.51	8.8				
		27.6	13.1	0.016	0.052	0.31	25.2				
			28.3	0.095	0.198	0.48	14.3				
			38.6	0.171	0.321	0.53	12.0				
			51.7	0.213	0.382	0.56	13.5				
			72.4	0.295	0.540	0.55	13.4				
		69.0	30.3	0.019	0.054	0.35	56.1				
			60.7	0.076	0.167	0.46	36.3				
			91.7	0.216	0.425	0.51	21.6				
	HS-12-3	6.9	3.4	0.002	0.009	0.22	37.8	1.435	31.41	97	
			7.6	0.005	0.026	0.19	29.2				
			9.7	0.009	0.042	0.21	23.1				
			13.1	0.017	0.070	0.24	18.7				
			20.0	0.038	0.118	0.32	16.9				
		27.6	14.5	0.010	0.049	0.20	29.6				
			25.5	0.039	0.125	0.31	20.4				
			40.0	0.092	0.228	0.40	17.5				
			49.6	0.125	0.284	0.44	17.5				
			76.5	0.228	0.453	0.50	16.9				
		69.0	32.4	0.032	0.105	0.31	30.9				
			64.1	0.121	0.263	0.46	24.4				
			93.8	0.228	0.485	0.47	19.3				
			111.0	0.324	0.704	0.46	15.8				
		103.4	46.9	0.049	0.239	0.21	19.6				
			88.3	0.197	0.457	0.43	19.3				

Table BVI. Results of repeated-load triaxial tests on fully recovered silt.

Condition	Sample	Confining pressure (kPa)	Deviator stress (kPa)	Radial strain (%)	Axial strain (%)	Resilient Poisson's ratio	Resilient modulus (MPa)	Dry density (Mg/m^3)	Moisture content (%)	Saturation (%)	Test temperature (°C)
Unfrozen	HS-2	13.8	26.9		0.009		298.9	1.362	31.0	86	
		27.6	55.2		0.023		240.0				
		69.0	135.1		0.057		237.1				
		137.9	268.2		0.116		231.2				
		6.9	20.7		0.006		345.0				
		13.8	44.8		0.046		97.4				
		27.6	83.4		0.080		104.3				
		69.0	203.4		0.190		107.1				
		137.9	388.9		0.263		147.9				
	HS-3	69.0	69.0		0.006		1150.0	1.482	28.4	94	
		137.9	135.8		0.093		146.0				
		13.8	40.7		0.056		72.7				
		27.6	81.4		0.140		58.1				
		69.0	196.5		0.212		92.7				

Table BVI. Results of repeated-load triaxial tests on fully recovered silt.

Condition	Sample	Confining pressure (kPa)	Deviator stress (kPa)	Radial strain (%)	Axial strain (%)	Resilient Poisson's ratio	Resilient modulus (MPa)	Dry density (Mg/m^3)	Moisture content (%)	Saturation (%)	Test temperature (°C)
Unfrozen	HS-4	27.6	27.6		0.018		153.3	1.357	30.1	83	
		69.0	69.0		0.012		57.5				
		137.9	134.5		0.118		114.0				
		6.9	20.0		0.006		333.3				
		13.8	40.0		0.046		87.0				
		27.6	80.0		0.144		55.6				
	HS-5	13.8	13.8		0.006		230.0	1.349	29.1	79	
		27.6	27.6		0.038		72.6				
		69.0	69.6		0.108		64.4				
		137.9	137.9		0.096		143.6				
		6.9	20.7		0.025		82.8				
		13.8	41.4		0.083		49.9				
		27.6	83.4		0.158		52.8				
		69.0	204.1		0.234		87.2				

APPENDIX C. REGRESSION EQUATION COEFFICIENTS FOR RESILIENT MODULUS AND POISSON'S RATIO FROM REPEATED-LOAD TRIAXIAL TEST DATA ON ASPHALT CONCRETE AND SILT

Resilient property (M_r in kPa)	Constant	Stress or material parameter: w (%)	w^2 $(\%)^2$	γ_d (Mg/m^3)	γ_d^2 $(Mg/m^3)^2$	σ_3 (kPa)	σ_3^2 $(kPa)^2$	σ_d (kPa)	σ_d^2 $(kPa)^2$	σ_1/σ_3	$(\sigma_1/\sigma_3)^2$	θ (kPa)	θ^2 $(kPa)^2$	T (°C)	T^2 $(°C)^2$	R^2 -	Standard error
	Regression coefficients: a_0	a_1	a_2	a_3	a_4	a_5	a_6	a_7	a_8	a_9	a_{10}	a_{11}	a_{12}	a_{13}	a_{14}		
Frozen Hanover Silt																	
M_r	-3.046×10^{8}	-	-	-	-	7.955×10^{6}	-4.592×10^{4}	-	-	+	+	+	+	3.100×10^{7}	7.432×10^{6}	0.539	3.108×10^{7}
M_r	-4.931×10^{6}	-	-	-	-	+	+	+	+	-	-	-	-	-	2.259×10^{6}	0.375	3.474×10^{7}
ln M_r	6.844×10^{1}	-	-8.008×10^{-3}	-33.267	-	-	-	-7.106×10^{-3}	7.652×10^{-6}	+	+	+	+	-6.620×10^{-1}	-	0.874	0.513
ln M_r	6.224×10^{1}	-	-7.377×10^{-3}	-29.266	-	+	+	+	+	-	-	-1.938×10^{-3}	-	-6.460×10^{-1}	-	0.853	0.544
Thawed Hanover Silt																	
M_r	-2.194×10^{5}	-	-	2.496×10^{4}	-	5.146×10^{2}	-	-2.772×10^{2}	-	+	+	+	+	+	+	0.294	2.110×10^{4}
M_r	-1.556×10^{5}	-	-	1.723×10^{5}	-	+	+	+	+	-4.835×10^{4}	7.991×10^{3}	5.651×10^{1}	-	+	+	0.280	2.140×10^{4}
ln M_r	-5.765×10^{1}	2.841	-3.984×10^{-2}	1.219×10^{1}	-	1.484×10^{-2}	-	-4.973×10^{-3}	-	+	+	+	+	+	+	0.464	0.597
ln M_r	-5.891×10^{1}	2.997	-4.208×10^{-2}	1.236×10^{1}	-	+	+	+	+	-1.232	2.010×10^{-1}	2.377×10^{-3}	-	+	+	0.473	0.595
μ_r	2.406×10^{1}	-1.146	1.556×10^{-2}	-	-1.454	-	-	-	-	+	+	+	+	+	+	0.122	0.270
μ_r	2.406×10^{1}	-1.146	1.556×10^{-2}	-	-1.454	+	+	+	+	-	-	-	-	+	+	0.122	0.270
ln μ_r	5.150×10^{1}	-2.67	3.690×10^{-2}	-	-2.528	-	-5.119×10^{-5}	6.084×10^{-3}	-	+	+	+	+	+	+	0.233	0.486
ln μ_r	5.364×10^{1}	-2.871	3.986×10^{-2}	-	-2.421	+	+	+	+	9.263×10^{-1}	-1.671×10^{-1}	-	-	+	+	0.202	0.496
Unfrozen Hanover Silt																	
M_r	-7.198×10^{5}	-	-	-	5.050×10^{5}	1.483×10^{4}	-7.617×10^{1}	-6.234×10^{3}	1.189×10^{1}	+	+	+	+	+	+.	0.485	1.842×10^{5}
M_r	-3.304×10^{5}	-	-	-	4.581×10^{5}	+	+	+	+	-9.473×10^{4}	-	-	-	+	+	0.313	1.995×10^{5}
ln M_r	6.808	-	-	3.776	-	-	-	-	-	+	+	+	+	+	+	0.181	0.734
ln M_r	1.127×10^{1}	-	-	4.375	-	+	+	+	+	-	-6.060×10^{2}	-	-	+	+	0.350	0.667
Unfrozen Asphalt Concrete																	
M_r	7.734×10^{6}	-2.768×10^{5}	-	-	-	-	-	6.875×10^{3}	-	+	+	+	+	-6.542×10^{5}	1.254×10^{4}	0.856	3.86×10^{5}
ln M_r	16.4667	-0.4064	-	-	-	-	-	2.293×10^{-3}	-	+	+	+	+	-0.1797	1.856×10^{-3}	0.91	0.264

Note: - means the variable was entered in the regression analysis but was found to be not significant

+ means the variable was not entered in the regression analysis

APPENDIX D. DETAILED PROCEDURES FOR REPEATED-LOAD TRIAXIAL TESTING*

I. Mounting of specimens and measurement devices:

1. Have sides and ends of test specimens smooth and parallel.

2. If frozen test is to be performed first, have *all* equipment stabilized at test temperature.

3. Place the three target segments (~ 1 in. x 2 in. each) around the sample at mid height (use heavy gage aluminum foil) between the sample and the triaxial membrane. If the sample is stiff, place the membrane on it first, fold or roll it down halfway and then place the target segments. Perform this operation on the cell pedestal with porous stones and end caps in place.

4. Once the targets are placed, secure the ends of the membrane with O-rings to the top cap and the pedestal. (Care must be taken to position the targets so that the variable impedance transducers (VIT's) will line up roughly with the target center; placement too close to the edges of target will cause erroneous readout.)

5. Mounting of the linear variable differential transformer (LVDT) clamps:

a. Choose the stiffest spring that will not damage the sample. Place double-faced masking tape on the contact surfaces of the clamps.

b. Mark the third points of the sample on the membrane.

c. Place the lower clamp with the spring located between the two LVDT mounting rods.

d. Place the upper clamp in the same manner as the lower one, but rotated slightly (~ ¼ in.) clockwise to allow some clearance for the lower LVDT barrels when installed.

e. It will be necessary to make some fine adjustments on the clamps to achieve a uniform gage length.

f. Once the clamps are in place, install the LVDT mounting rods.

6. Installation of the LVDT's :

a. Install lower pair with *lead wires down.* Position the barrels for a zero output.

b. Install the upper pair with *lead wires up.* Position the barrels for a zero output. (Each core must be matched with its own barrel; serial numbers are noted on the clamps. Also, each LVDT must be matched with its proper input in the averager circuit.)

c. Measure the gage length over each pair of contacts.

7. Mounting of the multi-VIT's:

a. Measure the distance from the cell base to the center of the foil targets (slightly below center if sample is expected to deform greatly).

b. Adjust the multi-VIT sensors to the distance from the cell base determined in (a).

c. Make sure that micrometers for each sensor are fully retracted. Tighten (but not completely) the sealing grips for each sensor lead.

d. Carefully slide the cylinder over the sample taking care not to hit the LVDT's or the sample. It is necessary to feed the two LVDT connectors through the cylinder before sliding it down over the sample.

e. Once this is accomplished, check the alignment of the sensors on the targets. Then, using the micrometers, position the sensors (approximately 0.1 in. from the target).

f. Connect the LVDT leads (and thermocouple) to the top of the cell; install tie rods and tighten evenly.

g. Check the readout of each system to ensure proper connections, etc.

II. Set-up and operation of testing machine:†

1. Install shearing device on ram (~ 150 lb per cross section of synthetic dowel) for protection of load cell.

2. Position cross head (with ram fully extended) so that the triaxial cell itself is out of range of the ram, and the only possible contact is with the cell piston. (Thus, if an error should cause the ram to extend fully, no damage will result after the shear pins fail.)

3. Have the machine at operating temperature for these tests. Using the Function Generator (in span I), and operating in STROKE CONTROL (in range I), input a high amplitude sine or saw-tooth function at about 1 cps for 20 to 30 minutes. It is then necessary to turn the machine off and switch to LOAD CONTROL for the test.

4. Have the Data Trak on, but not cycling. *It must be in span II.*

5. Outer loop gain control must be set at 1 for the 500-lb load cell, and 1½ to 2 for the 200-lb load cell. If oscillations occur, lower this gain control very gradually until system becomes stable. Outer loop stability should be at 7 or 8.

* Note: all units are expressed in the English system because the load and displacement equipment used are calibrated in that system.

† Section II refers to the use of the model 810 testing machine by MTS Systems Corporation.

6. Data Trak operation and load cell considerations:

a. The Data Trak output has an amplifier which brings the maximum output (for the waveform used here) from about +0.5 v to 10.0 v and reverses polarity. The span II control admits this command signal to the feedback loop in proportion to its setting (0-00 to 10-00).

b. The MTS machine is set to provide 10-v excitation for the load cell. A 200-lb capacity load cell provides ± 10-v output full scale; therefore the feedback loop receives ± 10,000-mv/200-lb or ± 50-mv output for each pound of load applied. (For these tests, operation is in compression exclusively, so all voltages will be negative.) By the same token, the machine will respond with 1 lb of compressive load for every – 50 mv from the span II input control. So, to obtain a load of say 100 lb, (100 lb) x (– 50 mv/lb) or a – 5-v input is required. To obtain this, set the span II control at 5-00 (some fine adjustments will usually be needed to obtain the exact output from the load cell). For a 30-lb load, (30-lb) x (– 50-mv/lb) or – 1500-mv input is required. Set span II at 1-50 and adjust as required to obtain desired load cell output.

c. When the 500-lb load cell is used, ± 10,000 mv/500 lb or ± 20 mv/lb results. A 200-lb load would require (200-lb) x (– 20-mv/lb) or a – 4-v command signal. To obtain this, set the span II control at 4-00, and make fine adjustments. The span II setting may also be viewed on a percentage basis; that is, whatever percentage of the full load is desired is the percentage of full span required. A 50-lb load using a 200-lb load cell is 25% of the full load range; and 25% of the span results in a setting of 2-50. Note: It is always necessary to have the proper Gain Range Card installed in the D.C. conditioner. Each card is associated with a particular load cell.

7. Once the cell is fully prepared, set the meter on the controller panel to monitor load, and press lightly on the cell piston. The indicator should deflect to the left, indicating a compressive load.

8. Have the load recording channel positioned so that a slight dead load (0.5 lb) is required to zero the recording pen on a convenient line (usually to the right of the paper, since the load signal is negative and thus deflects to the left).

9. Raise the ram using the set point control. Over 5-00 places a *tension* demand on the system, so the ram retracts (goes up) seeking a tension load on the transducer. Since the set-up does not provide any means of applying tension to the load cell, the ram merely goes up to its limit and stays there. A setting of under 5-00 places a compression demand on the system. The ram extends (goes down) until this demand is found, via feedback from the load cell. The low gain settings required in the use of the low-range load cells used here result in a rather sluggish response to the set point command signal. (It is best for the operator to get a feeling for the ram's behavior by experimenting with the set point control while there are no obstacles in the way of the ram.) Center the triaxial cell and *gradually* lower the ram into contact with the cell piston. This must be done very slowly to avoid any impact on the apparatus. Once contact is made, monitor the load cell output and adjust the set point until the desired dead load is obtained.

10. Have all recording channels adjusted properly and sensitivities, calibration factors, sample number, date, etc., recorded on the chart paper. Set the confining pressure and allow temperature to stabilize.

11. When first testing a sample (especially if the material is stiff) begin with the span II *completely off* (0-00). Turn the Data Trak on and allow to cycle. Gradually turn the span control up to obtain the desired load. This is done because the system may require some adjustments at higher loads to prevent oscillations. If these levels of instability are approached gradually, the load cell output will show increasing levels of oscillations before the situation is serious enough to cause the machine to shut itself off. This allows the operator to lower the gain settings as required without interrupting the test.

12. Proceed with the test, changing the deviator and confining stress levels as required. (A table of all stress levels, span II setting and load cell output trace amplitudes should be prepared prior to testing.)

13. At the conclusion of the test, turn off the Data-Trak when the command signal is zero.

14. Raise the ram using the set point, slide the triaxial cell out from under the ram and then lower it to full extension.

15. Turn machine off if it is not to be used in the near future.

16. Final measurements:

a. Take final gage length measurements before removing LVDT's.

b. Record all final dimensions of sample, and obtain diameter measurements at the Multi-VIT target sites.

c. If sample is very soft or badly deformed, measure diameters with membrane and targets in place and subtract their combined thicknesses to obtain sample diameters.

III. Calibration procedures:

1. LVDT's:

a. Make sure all LVDT's are connected without cores inserted.

b. The averaging circuits are equipped with trim pots for each LVDT. Adjust pots completely clockwise until click is felt, then back off five to ten turns.

c. Set the recorder to zero.

d. Mount a barrel and its core on the calibration jig and adjust the core to electrical zero.

e. Adjust the core to the desired full range.

f. Adjust primary gain control on oscillator-demodulator unit to result in desired full-scale output. (Use trim pot for fine adjustments.)

g. Rezero the core, and change to a more sensitive setting on the recorder. Move the core a convenient increment and check the output. Use the pot to bring this output to the desired calibration factor.

h. Repeat step (g) until all recording sensitivities to be used have been checked.

i. Install the mate of the first LVDT in the jig and use the same procedure as before, but *do not* adjust the gain control on the oscillator-demodulator again. If that is moved, it will be necessary to recalibrate the first LVDT. Use only the pot in the averaging circuit.

j. The second pair of LVDT's is done exactly as the first. Start by adjusting the main gain control for the first one of the pair, then use only the pot in the averager for subsequent adjustments. Note: It is necessary to adjust *all* LVDT's to exactly the same calibration factor because of the nature of the recording system.

2. Setting LVDT's for a given full-scale range: Note: A range of 0.250 in. full scale is useful for thawed soil where greater deformations are expected. A range of 0.125 in. full scale is useful for frozen soil and some pavements where small deformations are expected. (This results in a stronger signal and thus greater resolution.)

a. For 0.250-in. range: The signal conditioner (oscillator demodulator) has a maximum output of ± 2.50 v. It is shared by two LVDT's in this case, so effectively there is ± 1.25 v provided to each LVDT. There is a scaling adder circuit which combines the two outputs from the averagers electrically and gives the resulting signal a *gain of 2.* This is the final signal that is recorded. Thus, when the single LVDT is set at full scale (± 0.250 in.), the maximum output should be adjusted (via the gain control) to produce ± 2.5 v on the recorder. When both LVDT's of the pair are so adjusted, the maximum full scale output is ± 5.0 v. Thus, the calibration factor is k = 0.2500 in./5000 mv = 0.5×10^{-4} in./mv.

b. For 0.125-in. range: Set the gain to produce the ± 2.5-v output when the core is located ± 0.125 in. from the zero position in the barrel. This will give a final output of ± 5.0 v for ± 0.125-in. travel, or k = 0.125 in./5000 mv = 0.25×10^{-4} in./mv. Note: It is recommended that the LVDT calibration be checked frequently. Generally, variations of up to 4% have been tolerated. It is possible to obtain a good estimate of the calibration factor (if it has fluctuated considerably) by finding the value of k for each pair of LVDT's and then finding an average weighted $^2/_3$ in favor of the upper pair of LVDT's. (The average is weighted so because the upper pair generally produces an output of three times the magnitude of the lower pair.)

3. Multi-VIT's: The multi-VIT's maintain their calibration very well. However, they should be checked periodically, using a target of the same material used for the test. This target must also have the same shape (~ 1-in. radius of curvature) as that of the sample tested. The same jig is used here as for the LVDT's. (Adaptors are provided.) Set each Multi-VIT to 1×10^{-4} in./mv using the calibration procedure suggested by the manufacturer.